Forest Ecology and Management 580 (2025) 122476

Contents lists available at ScienceDirect

Forest Ecology and Management

journal homepage: www.elsevier.com/locate/foreco

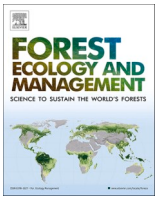

Synergistic negative effects of ash dieback and Armillaria root rot on health and stability of mature ash trees

Philipp Spiegel [a,b], Thomas Hintze [c], Aaron Kopp [a], Mario Sahli [a], Andreas Detter [d], Valentin Queloz [a], Simone Prospero [a], Renate Heinzelmann [a,*]

[a] Swiss Federal Research Institute WSL, Zürcherstrasse 111, Birmensdorf CH-8903, Switzerland
[b] Center for Microbiology and Environmental Systems Science, University of Vienna, Djerassiplatz 1, Vienna AT-1030, Austria
[c] Robinia Baumbüro, Aadorf CH-8355, Switzerland
[d] Brudi & Partner TreeConsult, Berengariastr. 9, Gauting D-82131, Germany

ARTICLE INFO

Key words:
Hymenoscyphus fraxineus
Armillaria spp.
Fraxinus excelsior
Basal stem necrosis
Static load test
Disease management

ABSTRACT

Since the early 1990s, the invasive pathogen *Hymenoscyphus fraxineus* has been spreading in Europe causing severe dieback of common ash (*Fraxinus excelsior*) and narrow-leaved ash (*Fraxinus angustifolia*). *H. fraxineus* also causes necrotic lesions at the stem base and on roots of ash trees, which frequently serve as an entry point of secondary wood decay fungi, like *Armillaria* spp. Rot of the stem base and roots leads to structural weaknesses of ash trees, which makes them prone to uprooting or stem fracturing during storm events. To prevent fatalities and damage to infrastructure it is crucial to timely identify and remove potentially hazardous ash trees. Here, we investigated the synergistic effects of *H. fraxineus* and *Armillaria* spp. on the health status (crown defoliation, presence, and extent of basal stem necroses) of mature trees of common ash in ten mixed forest stands in Switzerland over a four-year period (2018–2022). In addition, we conducted non-destructive static load tests on a set of 30 ash trees to assess their breaking and tipping stability so that stability weakness at the stem base could be related to tree health data. The health of the monitored ash trees declined rapidly during the monitoring period, indicating that also mature ash trees in mixed forests may be heavily impacted by ash dieback after prolonged exposure to *H. fraxineus* (here 12–13 years) and subsequent colonization by root rot pathogens. At the end of the monitoring, only 4.1 % of ash trees with a healthy crown (defoliation $\leq$ 25 %) remained and 75.4 % of ash trees showed basal stem necroses, which were, with a few exceptions, all colonized by *Armillaria*. Although the results from the static load tests indicated that predicting tree stability based on crown defoliation level and stem base damage level is not straightforward, i.e. also trees with advanced crown defoliation and stem necrosis can still be stable, our study shows that ash trees with necroses affecting at least 20 % of the basal stem circumference and trees with more than 75 % crown defoliation are likely to suffer from a weakness at the stem base. Building on the new findings and previous research, guidelines for the management of mature ash trees affected by ash dieback are suggested.

1. Introduction

Healthy and resilient forest ecosystems are crucial for biodiversity, carbon sequestration and ecosystem services (Watson et al., 2018). Various biotic stressors, including invasive pests (i.e., pathogens and insects), which are accidentally introduced mainly through global trade, as well as native harmful organisms that may emerge due to climate change, pose significant threats to tree species diversity and environmental sustainability worldwide (Santini et al., 2013; Teshome et al., 2020; Robbins et al., 2022). Globally, pathogens and insect outbreaks are responsible for the mortality of millions of trees, potentially increasing the global carbon release by forest ecosystems and also driving tree species (close) to extinction (Anagnostakis, 1987; Fensham and Radford-Smith, 2021; Quirion et al., 2021). In addition, huge, direct and indirect, economic costs may be associated with outbreaks of emerging and invasive pests (Eschen et al., 2023).

With a few exceptions (e.g. Manion, 1991), tree- and plant diseases historically have been considered to be caused by one single pathogen,

* Corresponding author.
E-mail address: renate.heinzelmann@wsl.ch (R. Heinzelmann).

https://doi.org/10.1016/j.foreco.2024.122476
Received 22 July 2024; Received in revised form 12 November 2024; Accepted 12 December 2024
Available online 8 February 2025

and synergistic effects of different organisms have been frequently neglected (Lamichhane and Venturi, 2015). However, there is an increasing number of tree decline symptoms that result from the synergistic interplay of different organisms, which concept is recognized as 'pathobiome' (Bass et al., 2019). For example, acute oak decline, which is widespread in Europe, is caused by the complex interaction of at least three bacterial species and a bark-boring jewel beetle (Denman et al., 2017). Similarly, local oak decline in Arkansas (USA) was attributed to the synergistic effect of a woodboring beetle and a root rot fungus (Kelley et al., 2009).

In Europe, a dramatic decline of common ash (*Fraxinus excelsior*) is observed, which is primarily caused by the invasive fungus *Hymenoscyphus fraxineus* (Ascomycota). The pathogen was most likely introduced from East Asia into north-eastern Europe (Poland, Lithuania) in the early 1990s and then rapidly spread throughout the entire distribution range of common ash (Gross et al., 2014; Carroll and Boa, 2024). Ash trees of all ages are affected and symptoms are necrotic lesions on leaves, which may extend to twigs and stems leading to wilting and dieback of girdled shoots (Gross et al., 2014). The defoliation of ash by *H. fraxineus* has physiological consequences for the tree (e.g. slower growth and reduced earlywood vessel size) which feeds back and amplifies crown dieback (Klesse et al., 2020). After infection, smaller and slow-growing trees can die within a few years, while larger and fast-growing trees may survive longer but suffer from severe structural weaknesses (Lenz et al., 2016; Klesse et al., 2020; Madsen et al., 2021). Although unexpected for a leaf pathogen, *H. fraxineus* may also cause necroses at the stem basis and at the root collar of ash trees (Husson et al., 2012). Previous studies have shown that such necroses are very often subsequently colonized by opportunistic fungal pathogens (Chandelier et al., 2016; Marçais et al., 2016; Enderle et al., 2017b; Madsen et al., 2021; Peters et al., 2023). The significant changes in the material properties of the colonized wood caused by these fungi, besides accelerating tree decline, may lead to potential structural collapses of standing trees, such as spontaneous or wind-induced stem breakage or uprooting (Cristini et al., 2024; Fuchs et al., 2024). Hazardous trees are particularly dangerous in urban environments or in forests with a prominent recreational function, as they may represent a risk for human life. Unfortunately, assessing mechanical stability of trees is difficult. On one hand, visual inspections are not completely reliable (van Wassenaer and Richardson, 2009; Pommnitz, 2016; Detter and Rust, 2018; Koeser et al., 2020). On the other hand, advanced technical inspections like drill resistance measurement (resistography) or acoustic tomography may help to assess the likelihood of stem fracture of trees affected by decay but cannot predict the likelihood of uprooting (Smiley et al., 2017; Xu et al., 2021). A valid alternative may be represented by non-destructive static load tests which have been applied in arboriculture since more than 35 years to assess tree stability against uprooting (Sinn and Wessolly, 1989; Sachverständigenarbeitsgemeinschaft (SAG) Baumstatik e. V., 2024), but are quite expensive and thus not best suited for testing a large number of trees.

Among the wood-decaying fungi frequently reported in basal stem necroses which were initiated by *H. fraxineus*, *Armillaria* species seem to play a major role (Chandelier et al., 2016; Marçais et al., 2016; Enderle et al., 2017b). The genus *Armillaria* (Basidiomycota) is cosmopolitan and currently includes over 40 described species (Heinzelmann et al., 2019; Kim et al., 2022). In Europe, five species are known to occur, namely *Armillaria mellea, A. ostoyae, A. gallica, A. borealis* and *A. cepistipes*, which differ in their geographical distribution, ecological behavior, host range, and pathogenicity (Guillaumin et al., 1993). While *A. mellea* and *A. ostoyae* can behave as primary pathogens on numerous tree species, *A. gallica, A. cepistipes*, and in most situations also *A. borealis*, are preferential saprotrophs with a low or weak pathogenic potential (Morrison, 2004; Prospero et al., 2004; Heinzelmann et al., 2017). Thanks to their efficient local spread via soil rhizomorphs and root contacts and their ability to exploit different woody resources (living trees, all kinds of dead wood), *Armillaria* individuals (so-called genets) can reach considerable sizes and persist over centuries in the same forest stand (Heinzelmann et al., 2019).

In this study, we aimed to assess the incidence of basal stem necroses on ash trees with symptoms of ash dieback and find criteria to identify potentially hazardous trees by comparing non-destructive static load test results (breaking and tipping stability) with tree health data, in particular crown defoliation, presence and extent of basal stem necroses, and presence of *Armillaria* spp. in the basal stem necroses. Investigations were performed in Switzerland where ash dieback was first observed in 2008 in the region of Basel (Engesser et al., 2009) and by 2015 it was already present all over the country (Queloz et al., 2017). The specific questions we addressed were: (1) Which is the incidence of basal stem necroses on ash trees with crown symptoms of ash dieback? (2) How frequent is *Armillaria* and which *Armillaria* species are present in basal stem necroses? (3) Are the basal stem necroses colonized by local *Armillaria* genets (i.e. already present in the stand) or newly arrived genets? And (4) Is it possible to predict tree stability by disease damage level indicators? Based on the results of our study, we formulated recommendations for a management of mature ash trees with ash dieback symptoms, aiming at minimizing the risk of stem breakage.

2. Materials and methods

2.1. Study sites and sampling strategy

The study was conducted at 47 sites (10 core sites, 37 additional sites) distributed across most of the distribution range of common ash in Switzerland and located at altitudes ranging from 200 to 968 m a.s.l. (Table 1, Supplementary Fig. S1a). All sites were characterized by mixed broadleaf forests with common ash (diameter at breast height (DBH) $\geq$ 20 cm) locally dominating. The sites were established in 2018 (30, including the 10 core sites) or 2023 (17) and initially included between 20 and 21 marked ash trees. Sites were selected for the presence of at least one seemingly resistant ash tree and the presence of at least 20 mature ash trees within a circle of up to 100 m radius. On the core sites, the coordinates of the marked trees were recorded, and this information was used to roughly estimate the plot size, i.e. the area covered by a polygon connecting the outermost ash trees, and the basal area of ash trees per ha (Table 1).

The 10 core sites were visited during summer (June to August) in the years 2018, 2020 and 2022. Of the initially 210 marked ash trees, 148 (10–19 trees per site) could be monitored for the entire study period. The 62 missing trees in 2022 (mainly hazardous or windfallen trees) were removed during the regular forest management. For this reason, windthrow of the ash trees could not be monitored reliably, and was not systematically recorded, although it occasionally occurred. In the first two monitoring years, crown defoliation (see below) and presence/absence of basal stem necroses was recorded. In 2022, the same monitoring was continued, but in addition the stem base and root collars and above ground woody roots of 10–18 ash trees (alive or died since the last inspection) per site (in total 138 ash trees across all sites) were thoroughly investigated for necroses whose extent was quantified as detailed below. In addition, the frequency of *Armillaria* in basal stem necroses (mycelium) and soil (rhizomorphs) was quantified.

The additional sites were visited either in August 2022 (1 site), April and May 2023 (9 sites) or July and August 2023 (27 sites) and the same basic monitoring of crown and stem health was conducted as on the core sites. However, for this study only *Armillaria* samples from basal stem necroses (1–3 trees per site) were considered.

2.2. Assessment of ash trees

2.2.1. Crown defoliation

Crown defoliation of ash trees was classified into the following six classes (adapted from (Lenz et al., 2012): Class 0: no defoliation (completely healthy crown), Class 1: 1–25 % defoliation, Class 2:

Table 1
Location of the ten core sampling sites and their characteristics (diameter at breast height (DBH) of ash trees, plot size, basal area of ash trees pro ha) in 2018 when the plots were established. In addition, the DBH of the subset of ash trees assessed in 2018, 2020 and 2022 is provided.

			At plot establishment				Trees assessed in 2018, 2020 and 2022	
Sampling site	Coordinates WGS84 (longitude, latitude)	Altitude (m a.s.l.)	No. of trees[a]	Mean DBH 2018 and range (cm)	Plot size (ha)[b]	Basal area pro ha (m^2/ha)[b]	No. of trees	Mean DBH 2018 and range (cm)
Aadorf	8.90103, 47.47120	647	21	30.8 (21–40)	0.13	12.05	14	33.2 (25–40)
Bäretswil	8.86581, 47.33121	775	21 (20)	33.6 (21–53)	0.21	8.75	16	33.4 (21–47)
Bassersdorf	8.62502, 47.45758	522	21	31.6 (20–50)	0.37	4.74	19	30.5 (20–50)
Bürglen	9.14062, 47.54675	436	21 (20)	34.0 (20–62)	0.30	6.21	19	33.1 (20–62)
Eschlikon	8.96804, 47.45746	571	21 (19)	24.1 (20–30)	0.13	6.86	14	24.3 (20–30)
Frauenfeld	8.87912, 47.57624	386	21 (14)	37.4 (22–73)	–	–	13	40.5 (27–73)
Homburg	8.98932, 47.62768	568	21 (11)	36.0 (20–60)	–	–	10	45.5 (21–60)
Kesswil	9.30517, 47.58424	465	21 (19)	34.1 (20–43)	0.18	10.47	17	35.1 (20–43)
Quarten	9.22327, 47.11110	455	21	27.4 (20–36)	0.10	12.22	11	28.2 (21–36)
Uster	8.69759, 47.35105	454	21 (16)	38.0 (21–96)	0.18	15.41	15	36.9 (21–72)
Total	–	–	210	–	–	–	148	–

[a]In parentheses the number of trees with individual coordinates. These trees were used to obtain a rough estimate of the plot size and the basal area pro ha.
[b]The plot size and the basal area pro ha were estimated based on the trees with individual coordinates only. The plot size was estimated as the area covered by a polygon connecting the outermost trees per plot. No estimate is provided if more than five trees were lacking coordinates on a sampling site.

26–50 % defoliation, Class 3: 51–75 % defoliation, Class 4: 76–99 % defoliation, Class 5: complete defoliation (dead tree). For the few additional sites visited in April or May 2023 crown defoliation was not estimated, because the trees were not yet foliated.

2.2.2. *Armillaria* assessment and sampling

The stem base (lower part of the trunk that transitions from trunk tissue to root tissue) of the selected trees was inspected for necrotic lesions as follows. First, the bark was visually checked for signs like swollen or sunken bark and sap flow. Then, to verify the presence of necrotic tissue, small cuts were made with a chisel to expose the underlying tissue. The extent of basal stem necroses was quantified as the percentage (5 %-steps) of basal stem circumference covered by all present necroses. In addition, the length of tallest necrosis per tree was measured. The root collars, defined here as the transition zones between the trunk and the woody roots, and above ground parts of the woody roots were also carefully checked for necroses, and their degree of damage was classified into the following six categories: Category 0: all root collars/above ground woody roots intact, Category 1: presence of one small necrosis ($\leq$ 50 % of root collar/woody root affected) on one root collar/above ground woody root, Category 2: presence of one large necrosis ($>$ 50 % of root collar/above ground woody root affected) on one root collar/above ground woody root or small necroses on two root collars/above ground woody roots, Category 3: presence of a large necrosis on two root collars/above ground woody roots or small necroses on three root collars/above ground woody roots, Category 4: presence of a large necroses on more than three root collars/above ground woody roots or small necroses on all root collars/above ground woody roots, Category 5: all root collars/above ground woody roots with large necroses or completely rotten.

If *Armillaria* was present in the basal stem necroses or necrotic root collar/above ground woody root tissue, a sample per tree was taken (Supplementary Fig. S1b). In most cases, mycelial fans were collected, but sometimes also rhizomorphs or decayed wood. For some trees also epiphytic rhizomorphs, or rhizomorphs present in the rhizosphere were sampled. Mycelial fans (approx. ½ cm^2) and wood tissue (approx. ¼ cm^3) were collected in 2 ml Eppendorf tubes, whereas rhizomorphs were collected in Ziploc bags. In the laboratory, rhizomorphs were washed with tap water and for each rhizomorph approx. 1 cm was cut into sections of 1–2 mm which were collected in a 2 ml Eppendorf tube and frozen at −20 °C until further processing. Other fungi eventually present in basal stem necroses were also sampled (mycelium, sporocarps or wood tissue).

To assess the abundance of *Armillaria* rhizomorphs in the forest soil, two holes with a surface area of approx. 15 × 15 cm and depth of approx. 10–20 cm were produced with a hand shovel at 1 m and 3 m from the stem, facing away from the most prominent basal stem necrosis, if present, or otherwise in a random direction (Supplementary Fig. S1b). If soil rhizomorphs were found in the soil sample removed from the hole, they were collected and further processed in the laboratory as described above. If no rhizomorphs were found in the soil sample, the hole was recorded negative for soil rhizomorphs.

2.2.3. Statistical analysis

Statistical analyses were conducted using the R software environment version 4.3.2 (R Core Team, 2023). Two-sided Fisher's exact tests were used to test for an association between crown defoliation class and the presence of basal stem necroses and between crown defoliation class and the presence of *Armillaria* in the basal stem necroses. The same test was used to compare the *Armillaria* species composition in basal stem necroses and soil. The correlation between the extent and lenght of necroses as well as between the frequency of *Armillaria* in soil and necroses was assessed using the Spearman rank correlation considering the data did not follow a bivariate normal distribution. The significance of the correlation was tested using an asymptotic test as implemented in the R package coin version 1.4–3 (Hothorn et al., 2006). The association of the crown defoliation class with the extent of necroses was tested using one-way ANOVA's. If the increase in mean extent of necroses from a crown defoliation class to the next one was statistically significant was assessed using contrasts as implemented in the R package multcomp version 1.4–25 (Hothorn et al., 2008). The association of the crown defoliation class with the length of the tallest necrosis was tested using a Kruskal-Wallis test because normality of residuals was not given. To explore if the length of the tallest necrosis significantly increased from one crown defoliation class to the next one, Dunn's test was used. A Bonferroni correction was applied to *p*-values resulting from a multiple testing procedure.

2.3. Identification of *Armillaria* and other fungal species

Before DNA extraction, samples were lyophilized overnight. Afterward, a 3 mm steel bead was added to each tube and samples were mechanical sheared at 30 Hz for 2 min using a Mixer Mill MM 400 (Retsch GmbH, Haan, Germany). DNA was extracted using the sbeadex Plant DNA Purification Kit (LGC, Teddington, UK) on the KingFisher Flex Purification System (Thermo Fisher Scientific, Waltham, MA, USA).

For identification of *Armillaria*, the two following approaches were used. First, two PCRs with partially species-specific primers for the RNA

polymerase II gene (Cornejo et al., 2024) were performed using the primers: PCR1 (duplex): Aost-RPB2-F, Aost-RPB2-R, Amel-RPB2-F, Amel-RPB2-R, PCR2: Abor-RPB2-F, Abor-RPB2-R (Cornejo et al., 2024). In addition, the elongation factor 1 alpha (EF1α) gene was amplified using the primers EF1 595 F (Maphosa et al., 2006) and ArmEF1-α R (Mulholland et al., 2012). All PCR reactions were conducted in reaction volumes of 10 μL with final concentrations of 1x JumpStart REDTaq ReadyMix (Sigma-Aldrich, St. Louis, MO, USA), 0.2 μM of each primer (0.8 μM of Amel-RPB2-F and Amel-RPB2-R) and 2 μL of 10-fold diluted DNA template. PCR amplification was carried out as follows: initial denaturation at 94 °C for 2 min, 33 cycles (EF1α-PCR: 35 cycles) of 30 sec at 94 °C, 30 sec at 60 °C (EF1α-PCR: 55 °C), 1 min at 72 °C, and a final elongation for 10 min at 72 °C. Products of PCR1 and PCR2 were visualized on 1.5 % agarose gels using electrophoresis. The PCR products of the EF1α-PCR were then digested with Alu I (Fermentas, Waltham, MA, USA) according to manufactures instructions and the digested fragments visualized on 1.5 % agarose gels. Samples were assigned to *Armillaria* species based on the presence/absence and size of PCR products (PCR1, PCR2) and the size of the digested fragments (Alu I digest of EF1α PCR products) (Cornejo et al., 2024; Tsykun et al., 2013) (Supplementary Table S1).

Second, Sanger sequencing of the partial EF1α gene (same primers as above; for *Armillaria* samples) and the ITS region (primers ITS5 and ITS4, White et al. 1990; for non-*Armillaria* samples) was performed as follows. PCR-reactions with volumes of 25 μl with final concentrations of 1x GoTaq G2 Hot Start Green Master Mix (Promega, Madison, WI, USA), 0.4 μM of each primer and 2 μl of 10-fold diluted DNA were set up. The target regions were amplified with the following cycling parameters: denaturation for 2 min at 94 °C, 35 cycles of 30 s at 94 °C, 30 s at 52 °C (EF1α: 60°C), 1 min at 72 °C, and a final elongation for 10 min at 72 °C. Sanger sequencing of PCR products was done using the BigDye Terminator v3.1 Cycle Sequencing Kit (Thermo Fisher Scientific). Sequencing in both directions was performed on an Applied Biosystems 3500 Genetic Analyzer (Thermo Fisher Scientific). The obtained sequences were assembled and edited with CLC Main Workbench 22 (www.clcbio.com). For species identification, the consensus sequences were submitted to BLAST searches in the NCBI nucleotide collection (http://blast.ncbi.nlm.nih.gov).

The first approach was applied to all *Armillaria* samples from the core sites (218) and the second approach to the samples from the additional sites (60) and to 26 samples from the core sites to verify the species identification obtained by the first approach.

2.4. Assessment of the structure of Armillaria populations

2.4.1. Microsatellite genotyping

Armillaria samples from the core sites were genotyped at 11 microsatellite loci using primers from Prospero et al. (2010) and Baumgartner et al. (2009). Depending on the species, all or a subset of loci is amplified, and loci may or not be polymorphic (Supplementary Table S2). The loci were amplified in three multiplex reactions (reaction 1: Arm13, Arm15, Arm17, Am124; reaction 2: Arm05, Arm11, Arm16, Am109, Am111; reaction 3: Arm02, Arm09) in 10 μl volumes containing final concentrations of 1x Type-it Multiplex PCR Master Mix (Qiagen, Valencia, CA, USA), 0.1 μM of each primer, and 1 μl of 10fold diluted DNA. The microsatellite loci were amplified using the following PCR program: 95 °C for 5 min, followed by 27 cycles of 94 °C for 30 s, 54 °C for 90 s and 72 °C for 90 s, and a final extension of 60 °C for 30 min and 72 °C for 30 min. The forward primers were labelled with a fluorescent dye (FAM-blue or HEX-green) at the 5'-end and alleles were sized on an Applied Biosystems 3500 Genetic Analyzer using GeneScan 400HD ROX dye Size Standard or GeneScan 500 ROX dye Size Standard (Thermo Fisher Scientific) as the internal size standard. Alleles sizes were scored with GeneMapper Software 5 (Thermo Fisher Scientific). Loci which showed no, or very weak amplification the first time (excluding monomorphic loci), were repeated in simplex reactions and with 30 PCR cycles.

2.4.2. Population diversity and structure

Multilocus genotypes (MLGs) were compared among and within sampling sites. Samples with identical MLG were considered to belong to the same *Armillaria* individual (= genet). Richness of genets within sampling site was assessed by calculating the index of clonal richness R = (G – 1)/(N – 1) as suggested by Dorken and Eckert (2001) with G representing the number of MLGs per site and N the number of samples per site. The value R varies from 0, when all samples belong the same genet, to 1, when all samples belong to a different genet. Similarly, richness of genets was compared among necrosis and rhizomorph samples as well as among *Armillaria* species.

The heterogeneity of genets was assessed by calculating Simpson's complement D* (Gini, 1912; Peet, 1974) which describes the probability that two randomly taken samples belong to the distinct genets. Low values indicate low heterogeneity and high values high heterogeneity of gents.

Spatial structure of *Armillaria* populations was assessed by plotting the occurrence of genets on a map based on the coordinates of the sampled trees using ArcGIS Pro 2.4.0 (Esri Inc., Redlands, CA, USA).

2.5. Ash tree stability

2.5.1. Static load tests

In August 2022, for 30 ash trees at the sites Aadorf (10), Frauenfeld (10), Homburg (3) and Kesswil (7) the bending strength of the stem and the anchoring strength of the roots was assessed by conducting non-destructive static load tests following a standard protocol established in international arboriculture (Brudi and van Wassenaer, 2002; Wessolly and Erb, 2016; Sachverständigenarbeitsgemeinschaft (SAG) Baumstatik e.V., 2024). A pulling line was attached to the stem in the lower crown of the target tree and low, quasi-static forces were applied using an electric winch (PCW3000-Li, Portable Winch, Sherbrooke, QC, Canada) (Supplementary Fig. S2). The applied force was monitored using a digital dynamometer with a resolution of 0.1 kN and an accuracy of 0.3 kN (TreeQinetic, IML Electronic GmbH, Rostock, Germany). The tilting of the root plate was measured with two bi-axial digital inclinometers with a resolution of 0.001° and an accuracy of 0.002° (TreeQinetic), which were attached to the stem base with the axes of their sensors arranged orthogonally to the pulling direction (Supplementary Fig. S2). The strain (elongation or compression) of the marginal fibers of the lower stem was measured with 2–4 elastometers with a resolution of 0.1 μm and an accuracy of 1 μm (TreeQinetic), which span an observation length of 200 mm and were attached to the side of the stem opposing or facing the position of the winch. After each pulling experiment, the inclinometers and elastometers were shifted to other suitable positions. For each tree, elastometers were used to monitor fibre strains along the stem at different heights below 1.2 m (mean 0.52 m), in a few cases up to 1.65 m. The inclinometers were mounted at lateral positions at the stem base at the front or backside relative to the position of the winch. All trees were pulled multiple times (2 times: 11, 3 times: 16, 4 times: 2, 5 times: 1). For each tree, the tilting of the root plate was measured at 3–10 different root collar positions and the elongation/compression of the marginal stem fibers at 4–12 different positions. To avoid irreversible damage, the trees were pulled to a maximal inclination of 0.25° at the stem base and strains lower than 250 μm at all positions along the stem.

During each pulling experiment, the data measured by the dynamometer, inclinometers and elastometers were constantly monitored and recorded at a sampling rate of roughly 4 Hz using the software TreeQineticMeasure 5.0.0.6 (IML Electronics GmbH, Rostock, Germany), which resulted in 100–400 datasets containing the values of all sensors recorded at one instant. Additionally, the height of the anchor point in the tree, the load angle of the pulling line at maximum force, and the height of all sensors were measured to determine the load applied to the tree in terms of a bending moment (e.g. Brudi and van Wassenaer, 2002).

The data obtained were evaluated using the software Arbostat (Arbosafe GmbH, Gauting, Germany) that is designed to determine the stability of trees against stem fracture and uprooting from static load tests according to the Static Load Test Method (van Wassenaer and Richardson, 2009; Detter and Rust, 2013; Wessolly and Erb, 2016; Rust and van Wassenaer, 2017). For each inclinometer position, the critical load causing uprooting failure was predicted from the non-destructive range as implemented in Arbostat. Based on a generalized tipping behavior of trees (Wessolly, 1996; Detter and Rust, 2018), the strength of the anchorage is assessed from the lateral force required to generate an inclination of the stem base of 0.25° (Brudi and van Wassenaer, 2002; Detter et al., 2023). Likewise, for each elastometer position the critical load causing primary failure in the stem was estimated using Arbostat. In this case, the correlation of applied load and recorded fibre strains was extrapolated according to Hooke's Law to the proportional of limit fibre compression (Detter and Rust, 2013; Detter et al., 2015). Additionally, the theoretical bending strength of the stem at 1 m height was calculated using Arbostat based on basic mechanic stress equations for a beam with elliptical cross-section from the stem diameters measured at 1 m height and the compressive strength of green wood. The material properties required for those calculations were adopted from the Stuttgart Tables (Wessolly and Erb, 2016).

A wind load analysis was conducted for each tree to estimate the expected wind the tree would be subjected to during a storm event using Arbostat and a digital photograph of the tree. The procedure follows general standards for the assessment of wind actions on structures (EN 1991–1–4: 2010) and was adapted to open grown trees by introducing adequate aerodynamic drag factors for trees (Sinn and Wessolly, 1989; Detter and Rust, 2013; Wessolly and Erb, 2016).

2.5.2. Factors of safety

Arbostat allows to determine factors of safety by dividing the projected strength of the tree (i.e. critical loads causing uprooting or stem breakage) by the estimated wind load during a storm. A factor of safety of 2 indicates that the tree's resistance against failure is exactly twice the expected wind load during a storm. In an arboricultural risk assessment, trees with a factor of safety < 1.5 for uprooting and/or stem breakage are usually be considered at risk of failure during a storm in order to accommodate for the inherent uncertainty of the analysis (Sachverständigenarbeitsgemeinschaft (SAG) Baumstatik e.V., 2024). The factors of safety were calculated for each sensor position on each individual tree. The lowest factor of safety for uprooting of a tree was considered to represent the tipping stability (TIS) of the tree, whereas the lowest factor of safety for stem breakage of a tree represented its breaking stability (BRS). The correlation between TIS and BRS was assessed using the Spearman rank correlation as described above.

To overcome the uncertainty involved in the estimation of wind loads on individual trees within the forest canopy (i.e., non-open grown trees) and the unknown effect of different degrees of defoliation on drag (Vollsinger et al., 2005), we did not identify trees with reduced stability solely based on their TIS or BRS but also considered the relative strength loss in the stem or anchorage by comparing TIS and BRS to a basic safety (BS). BS compares the potential load bearing capacity of a defect-free stem of the same dimensions and the projected wind load during a storm and was also calculated using Arbostat (Wessolly, 1995). A BS ≥ 1 indicates that a tree can bear the expected wind load during a storm. Comparing TIS and BRS with the BS indicates if a tree's load bearing capacity is reduced (i.e. if TIS $<$ BS and/or if BRS $<$ BS). Eventual errors in estimating the wind load do not betray the comparison because they equally affect all three factors of safety (Wessolly and Erb, 2016). If damage is present at the lower stem or in the anchorage below ground, BRS or TIS will deviate from BS regardless of the actual likelihood of failure during a storm (i.e. TIS ≥ 1.5 and BRS ≥ 1.5). A ratio TIS/BS < 1 or BRS/BS < 1 was used as an indicator of a weakened stem base and reduced tree stability for further statistical analysis.

We also used the factors of safety to estimate the bending strength of the tree stems as well as the anchorage strength of the root system. To obtain these properties, we multiplied BRS and TIS with the estimated wind load for each individual tree. Because the factors of safety represent the ratio of the strength (stem bending or anchorage) and the estimated wind load, the bending strength and anchorage can be obtained as described.

2.5.3. Association between tree stability and stem and crown damage severity

We tested for a statistically significant association between tree stability (trees weakened at the stem base vs. trees without indication of weakness, as defined above) and levels of basal stem damage severity expressed in four different ways (general stem base damage: no vs. yes, extent of basal stem necroses (i.e. percentage of basal stem circumference covered): < 20 % vs. ≥ 20 %, length of tallest necrosis: < 10 cm vs. ≥ 10 cm, rot of root collars and above ground woody roots: no vs. yes) and crown defoliation (26–75 % vs. 76–99 %) using two-sided Fisher's exact tests as implemented R version 4.3.2 (R Core Team, 2023).

In addition, we compared the relationship of stem strength (BRS * estimated wind load) with anchorage (TIS * estimated wind load) of ash trees with a low extent of basal stem necroses (< 20 %) and a higher extent (≥ 20 %) of basal stem necroses by fitting a linear model with an interaction term using the lm() function implemented in R.

3. Results

3.1. Ash dieback severity

Overall, the health status of the 148 ash trees at the core sites declined rapidly between 2018 and 2022 (Fig. 1, Supplementary Table S3). During this period, the proportion of trees with little crown defoliation (≤ 25 %, i.e. crown defoliation classes 0 and 1) decreased from 41.2 % in 2018 over 23.1 % in 2020 to only 4.1 % in 2022. An increase in crown defoliation was also observed at the site level. In 2018, the percentage of ash trees with ≤ 25 % crown defoliation ranged from 21.4 % (Aadorf) to 63.6 % (Quarten) (Supplementary Fig. S3). In 2022, this percentage dropped to 0.0 % on 6 sites and ranged between 5.3 % (Bürglen) and 14.3 % (Eschlikon) on the other sites.

In 2018, the recorded ash mortality rate across sites was 3.4 % (Fig. 1). At that time, seven sites showed no ash mortality at all, and at the other sites the mortality ranged from 6.7 % (Uster) to 11.8 % (Kesswil) (Supplementary Fig. S3). Four years later, already 19.6 % of the ash trees had died (Fig. 1), and just one site (Aadorf) showed no ash mortality. At the other sites, ash mortality ranged from 5.3 % (Bürglen) to 57.9 % (Bassersdorf) (Supplementary Fig. S3).

Similar as crown transparency, the proportion of trees with necroses at the stem base increased drastically over the 4-year study period, from 12.3 % in 2018 to 75.4 % in 2022 (Fig. 1). This corresponds to a more than 5-fold overall increase of trees with basal stem necroses within just four years. In 2018, all inspected ash trees at four sites were still free of basal necroses, whereas two years later all sites had trees with basal necroses (Supplementary Fig. S4). In 2022, at all sites at least 50 % of the ash trees had basal stem necroses, with the worst situation observed in Kesswil where all trees showed basal stem necroses.

In 2018 the correlation between the degree of crown defoliation and the presence of basal stem necroses was slightly significant (Fisher's exact test, $p = 0.036$, Fig. 1), i.e. defoliated trees had an increased chance to have basal stem necroses. From 2020 onwards, the correlation became considerably stronger (Fisher's exact test, 2020: $p = 5.7 \times 10^{-4}$, 2022: $p = 1.5 \times 10^{-4}$, Fig. 1).

3.2. Size of basal stem necroses

In 2022, the extent (width) of basal necroses estimated as the percentage of basal circumference covered by necroses was highly variable, ranging from 5 % to 100 % (Fig. 2, Supplementary Table S3). The length

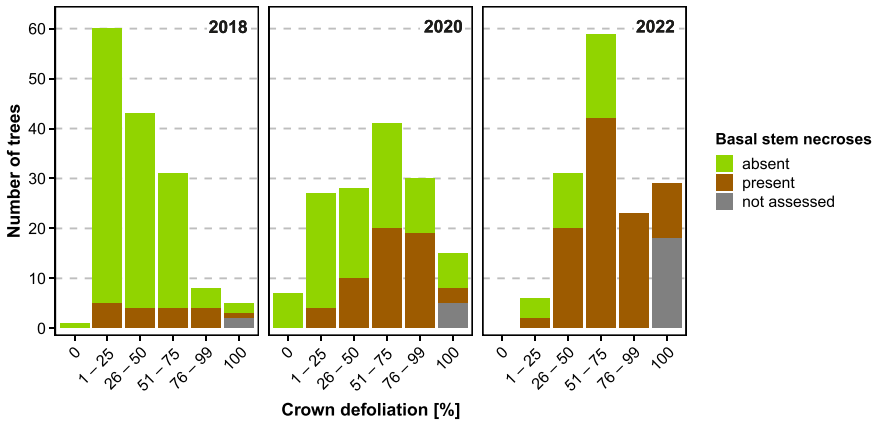

Fig. 1. Crown defoliation of 148 ash trees (*Fraxinus excelsior*) located on ten sampling sites (core sites) in northeastern Switzerland in the years 2018, 2020 and 2022 and the presence of basal stem necroses. Ash trees without basal stem necroses are indicated in green, and ash trees with basal stem necroses in brown. Trees where the presence of basal stem necroses was not assessed or assessable are indicated in grey. For example, if ash trees were dead (100 % crown defoliation) already in the previous assessment year, the presence of basal stem necroses was not assessed in the following assessment(s) years. Sometimes also heavy bark beetle infestation of the dead ash trees made it impossible to determine the presence/absence of basal stem necroses on dead trees.

of the necrosis longest in height along the main stem ranged from 1 cm to 190 cm (Supplementary Fig. S5a) and showed a moderate positive correlation with the extent of the necroses ($r_{Spearman}(82) = 0.59$, $p = 1.0 \times 10^{-7}$; Supplementary Fig. S5b). With increasing crown defoliation the extent of stem necroses generally increased even if within crown defoliation classes high variation was observed (one-way ANOVA, $F(4, 90) = 15.84$, $p = 7.5 \times 10^{-10}$; Fig. 2). The increase in necrosis extent from a crown defoliation class to the next class was statistically significant starting from defoliation class 3 (= 51–75 % defoliation) ($p = 1.5 \times 10^{-3}$ and $p = 2.2 \times 10^{-4}$; Fig. 2). The same trend was also observed for the maximal length of necroses (Kruskal-Wallis-Test, $\chi^2 = 9.788$, $p = 0.044$; Supplementary Fig. S5a). However, only the increase from defoliation class 3–4 was statistically significant ($p = 0.043$).

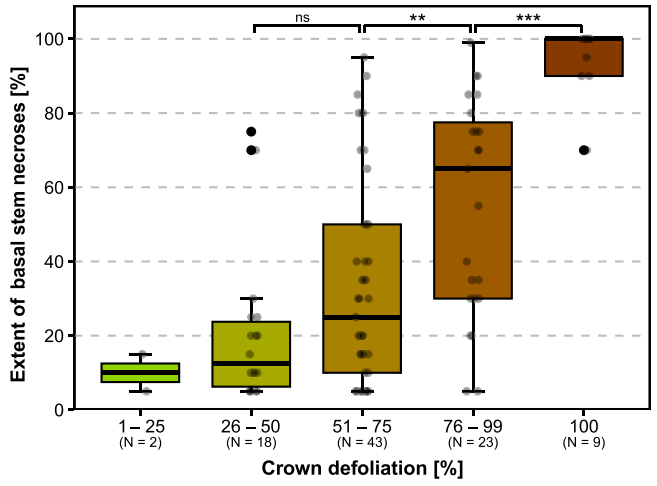

Fig. 2. Extent of basal stem necroses (= percentage of basal stem circumference covered by necroses) on ash trees (*Fraxinus excelsior*) in 2022 in comparison to crown defoliation. In each boxplot, the thick central line represents the median. The colored boxes span from the first (25th percentile) to the third quartile (75th percentile) and the whiskers extend maximally 1.5 times the distance between the first and third quartile from the box edges. The statistical significance of the increase in mean extent of necroses from one crown defoliation class to the next one, was assessed using contrasts. ns: not significant, **: p-value < 0.01, ***: p-value < 0.001, significance not indicated: no test conducted. To account for multiple testing, a Bonferroni correction was applied to p-values.

3.3. Stem necroses and Armillaria occurrence

3.3.1. Presence of Armillaria in basal stem necroses and rhizomorph density in soil

In 2022 most basal stem necroses (94.1 %) were colonized by *Armillaria* (Fig. 3) and the presence of *Armillaria* was not correlated with the degree of crown defoliation (Fisher's exact test, $p = 0.773$). At six sites, all investigated necroses were colonized by *Armillaria*, whereas at the other sites *Armillaria* was found in 62.5 % (Frauenfeld) to 92.3 % (Bürglen) of the necroses (Supplementary Fig. S6).

In 2022, the overall rhizomorph density in the soil (= percentage of soil samples with rhizomorphs) across all core sites was 34.1 % and varied strongly among sites (from 16.7 % in Bürglen and Frauenfeld to 69.2 % in Kesswil) (Supplementary Fig. S7). The presence of basal stem necroses was positively correlated with the rhizomorph density in the soil ($r_{Spearman}(10) = 0.7$, $p = 0.022$; Supplementary Fig. S7).

In 2022, epiphytic rhizomorphs were found at the stem base of

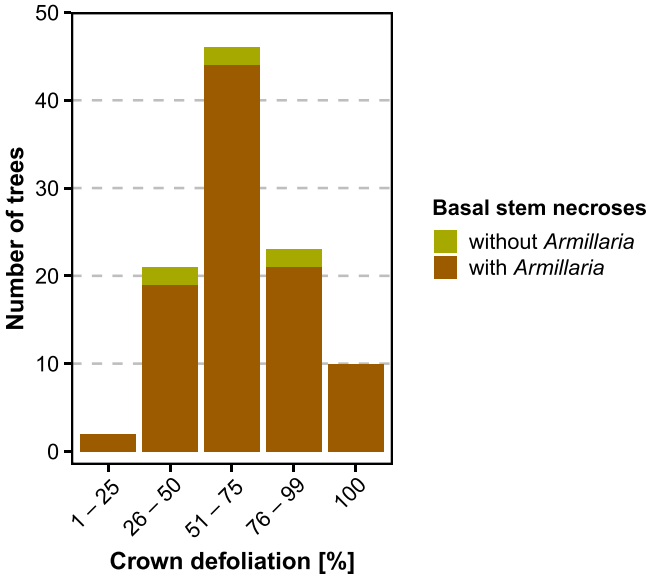

Fig. 3. Presence of *Armillaria* spp. in basal stem necroses of ash trees (*Fraxinus excelsior*) in 2022 in comparison to crown defoliation. The presence of *Armillaria* was confirmed either by finding mycelial fans or rhizomorphs in the necroses and/or molecular methods. *Armillaria* present (olive green), *Armillaria* not present (brown).

roughly half (54.4 %) of the 136 inspected ash trees. Ash trees with stem necroses were more likely to have epiphytic rhizomorphs than trees without necroses (62.0 % of 100 trees vs. 33.3 % of 36 trees; Fisher's exact test, $p = 3.6 \times 10^{-3}$).

3.3.2. *Armillaria* species diversity

A total of 203 out of 218 (93.1 %) *Armillaria* samples collected from ash trees and soil at the core sites were successfully identified to species: most of them (97.5 %) belonged either to *A. gallica* (104 samples) or *A. cepistipes* (94 samples), whereas three samples belonged to *A. mellea* and two samples to *A. borealis* (Fig. 4, Supplementary Table S3). The latter two species were only present in stem necroses on ash trees. The prevalence of *A. cepistipes* and *A. gallica* in the soil was not affected by the distance (1 m vs. 3 m) to the ash tree (Fisher's exact test: $p = 1.000$, Fig. 4). In tree necroses, *A. gallica* was clearly more common than *A. cepistipes* (66.7 % vs. 33.3 %) whereas in the soil (1 m and 3 m combined) the opposite was observed (40.4 % vs. 59.6 %) (Fisher's exact test: $p = 7.6 \times 10^{-4}$, Fig. 4). At the additional sampling sites, the same *Armillaria* species as at the core sites were detected, except *A. borealis*, which was not found (Supplementary Table S4). Across those sites *A. gallica* and *A. cepistipes* were almost equally represented (41.7 % vs. 45.0 %) whereas *A. mellea* remained a rare species (13.3 %).

Regarding the geographic distribution of the *Armillaria* species associated with basal stem necroses (core and additional sites combined), *A. cepistipes*, *A. gallica* and *A. mellea* were found widely distributed across Switzerland, whereas *A. borealis* was only sampled at two sites (Bäretswil and Eschlikon) in northeastern Switzerland (Fig. 5a, Supplementary Table S4). The altitudinal distribution of the species, however, showed clear differences (Fig. 5b). At altitudes below 400 m a.s.l. only *A. gallica* and *A. mellea* were found. *Armillaria cepistipes* only started to occur at altitudes above 400 m a.s.l. but, unlike *A. gallica* and *A. mellea*, remained frequent also above 600 m a.s.l. The two records of *A. borealis* were both from altitudes above 550 m a.s.l.

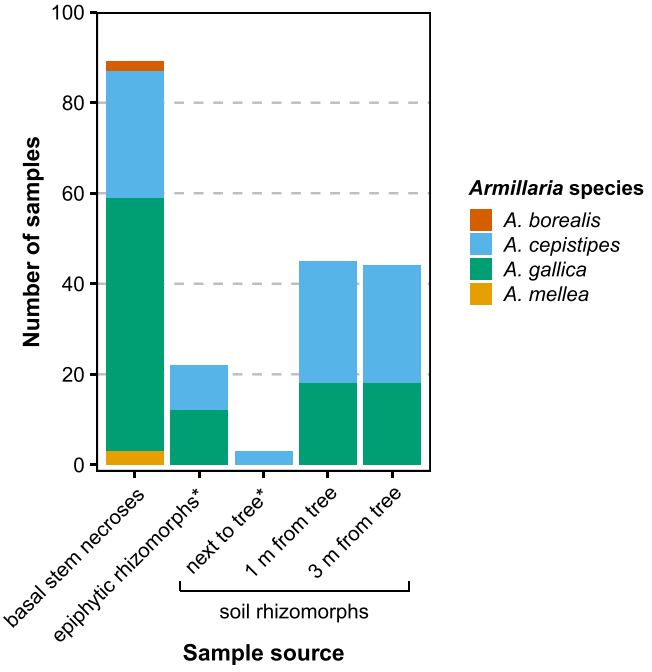

Fig. 4. Occurrence of *Armillaria* species in different ecological niches on and around ash trees (*Fraxinus excelsior*). Samples were collected from basal stem necroses, from the outside of the bark (epiphytically growing rhizomorphs), from the soil next to the tree and in 1 m and 3 m distance of the tree. * samples were not collected systematically.

3.4. Other fungal species in basal stem necroses

At the stem base of the investigated ash trees, we occasionally found lesions or fruiting bodies of fungal species belonging to the Ascomycete genera *Neonectria* and *Thelonectria* and the Basidiomycete genera *Gloiothele*, *Physisporinus* and *Coprinus* (Supplementary Table S5). Those species always co-occurred with *Armillaria* on the same tree.

3.5. Genetic structure of Armillaria populations

In total, 191 *Armillaria* samples (84 mycelium/rhizomorphs from basal stem necroses, 90 rhizomorphs from the soil and 17 rhizomorphs growing epiphytically on the stem base) collected at the ten core sites were successfully genotyped with microsatellite markers. Altogether, 41 different genets were identified (Supplementary Table S6). All genets were unique to a sampling site. Overall, genet diversity was higher in samples from basal stem necroses than in rhizomorph samples from the soil (genet richness (R): 0.39 *vs.* 0.29). More than half of genets (58.5 %) were represented by two or more samples. In line with the dominance of *A. gallica* and *A. cepistipes* at the ten core sites, most genets were attributed to those two species (*A. cepistipes*: 20, *A. gallica*: 16). Noteworthy, genet diversity was higher in *A. cepistipes* than *A. gallica* (R: 0.22 *vs.* 0.16). The rare species *A. mellea* and *A. borealis* had three and two genets, respectively.

The number of *Armillaria* genets identified per site ranged from one (Homburg) to 7 (Eschlikon) (Table 2, Supplementary Table S6). Genet richness and heterogeneity varied considerably among sites, with the index of clonal richness ranging from 0.00 (Homburg) to 0.33 (Frauenfeld) and Simpson's complement ranging from 0.00 (Homburg) to 0.82 (Eschlikon).

The identified genets were highly variable in size (Fig. 6, Supplementary Figs. S8 to S15, Table 2, Supplementary Table S7). On one side, genets of *A. mellea* and *A. borealis* were only represented by one sample and restricted to stem necroses. On the other side, individual *A. cepistipes* and *A. gallica* genets included 1–15 samples and 1–18 samples, respectively. In these two species, genets were associated with 1–7 trees and with 1–12 trees, respectively, and were found in basal stem necroses and/or as rhizomorphs. The largest five genets of *A. cepistipes* (9–15 samples each) and *A. gallica* (10–18 samples each) were present both in basal stem necroses and in the soil. For the largest five *A. cepistipes* genets, 11.1–40 % of samples were from stem necroses, whereas for the five largest *A. gallica* 50–61.5 % of samples were from stem necroses (Supplementary Table S7).

3.6. Stability of ash trees

The basic safety (BS) of the 30 assessed ash trees ranged from 1.3 to 4.2, indicating that the stem of all trees have reached sufficient diameters to potentially bear the expected wind load during a storm ($BS \geq 1$). However, 5 trees did not reach the required threshold of 1.5, even if only one of them presented a potential failure risk during a storm (Supplementary Fig. S16, Supplementary Tables S8 and S9). The tipping and breaking stability were strongly correlated ($r_{Spearman}(28) = 0.81$, $p = 1.2 \times 10^{-5}$). The ratio of TIS/BS and BRS/BS is indicating that nine trees may have a weakness at the stem base (i.e. TIS/BS < 1 and BRS/BS < 1; Supplementary Fig. S17). Eight of them showed basal stem necroses and a crown defoliation (26–50 %: 2 trees; >50 %: 6 trees). One tree had heavy stem damage by a forestry vehicle and a crown defoliation between 26 % and 50 % (1 tree) (Table 3). Six of these trees were at risk to be uprooted or broken during a storm (i.e. TIS < 1.5 and/or BRS < 1.5; Supplementary Fig. S16), assuming the effect of crown defoliation on drag in a storm would not reduce the wind loads too much. Trees with an undamaged stem base (no necroses, no damage by forestry vehicles) did not show any weakness at the stem base (Fig. 7). Trees with minimal amounts of necrotic tissues (total extent of necroses < 20 % of basal stem circumference, length of tallest necrosis < 10 cm) and low or

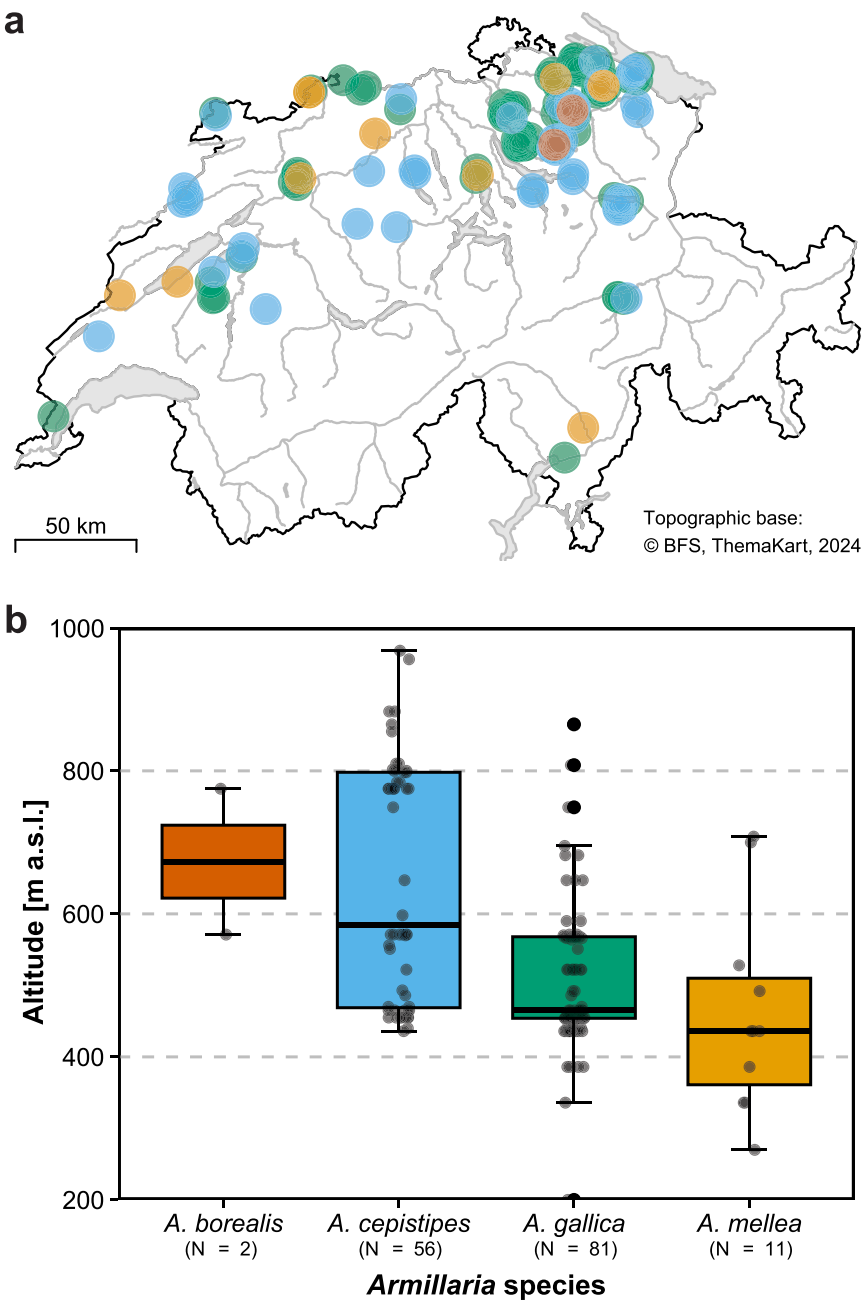

Fig. 5. Geographic (a) and altitudinal (b) distribution of the four *Armillaria* species sampled from basal stem necroses on ash trees (*Fraxinus excelsior*) on 47 sampling sites (10 core sites, 37 additional sites) across Switzerland. In each boxplot, the thick central line represents the median. The colored boxes span from the first (25th percentile) to the third quartile (75th percentile) and the whiskers extend maximally 1.5 times the distance between the first and third quartile from the box edges. Dark orange: *A. borealis*, light blue: *A. cepistipes*, green: *A. gallica*, orange: *A. mellea*.

moderate crown defoliation ($\leq$ 75 %) rarely showed signs of a weakness at the stem base (Fig. 7). Generally, with increasing damage severity of crown and stem base the proportion of trees with a weakness at the stem base increased. However, a statistically significant association with weakness at the stem base was only observed for the extent of basal stem necroses ($<$ 20 % vs. $\geq$ 20 %, Fisher's exact test: $p = 0.013$) and for the degree of crown defoliation (26–75 % vs. 76–99 %, Fisher's exact test: $p = 0.013$) (Fig. 7, Supplementary Table S10).

In addition, we observed that the relationship between stem strength and anchorage was different for trees where the necroses covered $<$ 20 % of the basal circumference and trees where the necroses covered $\geq$ 20 % of the basal circumference (Fig. 8). Not only differed the slopes of the regression lines significantly ($p = 0.004$), but also was the relationship closer to a 1:1 correlation for trees with necroses covering $<$ 20 % of the basal circumference (slope: 0.90) than for trees with a higher necroses level (slope: 0.60).

4. Discussion

4.1. Severity of ash decline

Monitoring of ash health in northeastern Switzerland over four years (2018–2022) in mature mixed ash stands revealed a rapid decline of ash trees, although considerable variation across the monitored sites was observed. When the monitoring was started in 2018, *H. fraxineus*, the invasive causal agent of ash dieback, had presumably already been

Table 2
Genetic diversity and heterogeneity of *Armillaria* populations on the ten core plots.

Sampling site	No. of samples	No. of genets per *Armillaria* species		No. of samples per genet	No. of trees associated with each genet[a]	Index of clonal richness (R)	Simpson's complement (D*)
Aadorf	15	*A. cepistipes*	1	9	7	0.14	0.56
		A. gallica	2	1, 5	1, 4		
		Total	3				
Bäretswil	20	*A. borealis*	1	1	1	0.21	0.69
		A. cepistipes	4	1, 3, 5, 10	1, 3, 4, 6		
		Total	5				
Bassersdorf	16	*A. cepistipes*	1	2	1	0.13	0.57
		A. gallica	2	4, 10	3, 7		
		Total	3				
Bürglen	18	*A. cepistipes*	2	1, 1	1, 1	0.29	0.62
		A. gallica	2	3, 11	2, 9		
		A. mellea	2	1, 1	1, 1		
		Total	6				
Eschlikon	30	*A. borealis*	1	1	1	0.21	0.82
		A. cepistipes	5	1, 4, 4, 4, 10	1, 3, 3, 4, 6		
		A. gallica	1	6	3		
		Total	7				
Frauenfeld	10	*A. cepistipes*	1	1	1	0.33	0.53
		A. gallica	2	1, 7	1, 3		
		A. mellea	1	1	1		
		Total	4				
Homburg	13	*A. gallica*	1	13	9	0.00	0.00
		Total	1				
Kesswil	30	*A. cepistipes*	4	1, 2, 4, 10	1, 1, 3, 7	0.17	0.73
		A. gallica	2	1, 12	1, 9		
		Total	6				
Quarten	20	*A. cepistipes*	1	15	7	0.16	0.43
		A. gallica	3	1, 1, 3	1, 1, 1		
		Total	4				
Uster	19	*A. cepistipes*	1	1	1	0.06	0.11
		A. gallica	1	18	12		
		Total	2				

[a]Includes samples from basal stem necroses, as well as soil samples. Soil samples were considered associated with the ash tree in which vicinity they were collected.

present for 8–9 years in the study area (Queloz et al., 2017). Although symptoms of ash dieback were common at all sites, at that time tree mortality across sites was still relatively low (3.4 %). Four years later, however, ash health had considerably deteriorated, with mortality observed by almost 20 % of the ashes. This is partially in contrast to what reported in young ash stands where high mortality rates were observed already a few years after exposure to the pathogen (Enderle et al., 2017a; Marçais et al., 2017). Older ash trees may also be affected by ash dieback, but usually their decline progresses slower as their physiological properties make them more robust (Lenz et al., 2016; Marçais et al., 2017; Klesse et al., 2020; Madsen et al., 2021). Likewise, in mixed forests with a low density of ash trees disease progression may be reduced (Grosdidier et al., 2020). However, our study shows that disease impact on mature ash trees present in mixed forests, can be heavy after a prolonged exposure to *H. fraxineus* (here 12–13 years) and successive root colonization by secondary pathogens. The high prevalence of ash trees showing basal stem necroses observed at the end of the monitoring period (75.4 %) is alarming and seriously questions tree survival.

4.2. Etiology of basal stem necroses

During the last monitoring of the core plots in 2022, when necroses were detected at the stem base of an ash tree, in most cases (94.1 %) the presence of *Armillaria* within necroses could be assessed either visually (presence of mycelial fans or rhizomorphs in the necroses) and/or with molecular methods. This confirms previous investigations showing that basal stem necroses on ash trees are often colonized by *Armillaria*, and other secondary fungi (Husson et al., 2012; Enderle et al., 2013, 2017b; Chandelier et al., 2016; Meyn et al., 2019; Madsen et al., 2021; Peters et al., 2023). As already mentioned in previous studies (Lygis et al., 2005; Bakys et al., 2011; Husson et al., 2012; Chandelier et al., 2016; Madsen et al., 2021), the prevalence of *A. gallica* and *A. cepistipes* which we observed in basal stem necroses strongly suggests that in this pathosystem *Armillaria* acts as a secondary pathogen. Noteworthy, common ash was not considered to be a main host for *Armillaria* species before the arrival of the ash dieback fungus in Europe (e.g. Drakulic et al., 2017; Gross et al., 2024). Thus, the invasive *H. fraxineus* seems to be able to increase the susceptibility of a native tree species to native root rot pathogens by weakening the host as well as by facilitating access to the host by the creation of necroses. Other fungi associated with rot at the stem base of ash trees included species of *Neonectria*, *Thelonectria*, *Gloiothele*, *Physisporinus* and *Coprinus* and they always co-occurred with *Armillaria* on the same tree. Except for *Neonectria* sp., which may also act as a parasite, all those species are saprotrophs and likely act as secondary colonizers. From the genus *Neonectria*, especially *N. punicea* is known as an early colonizer of root collar necroses on ash (Langer, 2017; Meyn et al., 2019; Karadžić et al., 2020; Peters et al., 2023) and also *Thelonectria* sp. was previously isolated from a stem necrosis on an ash tree (Peters et al., 2023). The absence of *H. fraxineus* in basal stem necroses in our study may relate to the sampling strategy and identification method, i.e. we may have missed it because we did not specifically sample and test for it using e.g. a specific detection method like qPCR (Ioos et al., 2009; Ioos and Fourrier, 2011). Also, if necroses are older and colonization by secondary fungi is highly advanced the detection of *H. fraxineus* may be hampered (Enderle et al., 2017a). An alternative explanation for not finding *H. fraxineus* in the basal stem necroses could also be that the necroses were initiated by *Armillaria* itself. The observed correlation between rhizomorph density in the soil and the rate of ash trees with basal stem necroses may indicate that *Armillaria* also contributes to necrosis formation in advanced stages of ash decline when trees are strongly weakened by *H. fraxineus*. However, additional investigations would be needed to support this hypothesis.

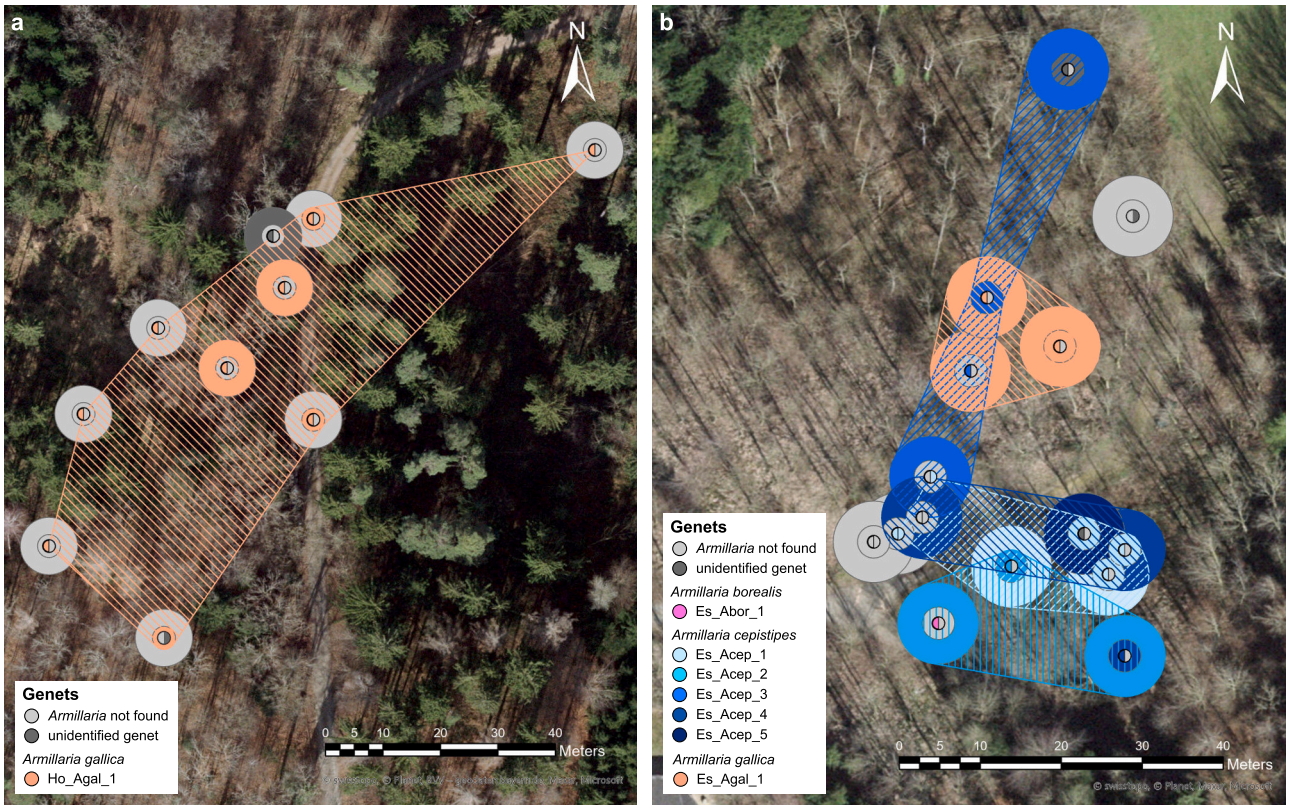

Fig. 6. Spatial distribution of *Armillaria borealis* (pink), *A. cepistipes* (blue shades) and *A. gallica* (orange) genets on the sampling site "Homburg" (a), which showed the lowest genet heterogeneity and on the sampling site "Eschlikon" (b), which showed the highest genet heterogeneity, in 2022. Dark grey shading indicates that *Armillaria* spp. was collected, but that genet identification failed, and light grey shading indicates that no *Armillaria* was found. Each circle represents a sampled ash tree (*Fraxinus excelsior*). The innermost circle represents samples collected from basal stem and root necroses (left half) and rhizomorphs growing epiphytically on the bark or in the soil next to the tree (right half). The outer circles represent rhizomorph samples collected from soil in 1 m and 3 m distance from the tree. For better visibility circles are not drawn to scale.

Table 3
Defoliation degree and type and extent of basal stem damage of ash trees (*Fraxinus excelsior*) with weakness at the stem base (TIS/BS < 1 and BRS/BS < 1) according to the conducted static load tests.

Tree ID	Stability[a]	Crown defoliation class (%)	Type of basal stem damage	Basal stem necroses		Damage degree of root collars and above ground woody roots
				Extent (%)[b]	Length of tallest necrosis (cm)	
1060a_3–02	TR/BR	51–75	Necrosis with *Armillaria*	20	94	small necrosis on 1 root collar/above ground woody root
1060a_3–05	BR	76–99	Necrosis of undetermined cause, no *Armillaria* present	20	–	–
1060a_3_08	–	76–99	Necrosis of undetermined cause, no *Armillaria* present	70	–	large necrosis on 2 root collars/above ground woody roots or small necroses on 3 root collars/above ground woody roots
1060a_3–11	TR	26–50	Heavily damaged by forestry vehicle	–	–	–
1060g_2–08	TR/BR	76–99	Necrosis with *Armillaria*	80	31	large necrosis on 2 root collars/above ground woody roots or small necroses on 3 root collars/above ground woody roots
1060g_2–17	TR	51–75	Necrosis with *Armillaria*	30	41	small necrosis on 1 root collar/above ground woody root
1060n_4_02	–	26–50	Necrosis with *Armillaria*	10	8	all root collars/above ground woody roots intact
1060n_4_07	–	26–50	Necrosis with *Armillaria*	25	26	small necrosis on 1 root collar/above ground woody root
1060u_4–02	TR/BR	76–99	Necrosis with *Armillaria*	90	120	large necroes on > 3 root collars/above ground woody roots or small necroses on all root collars/above ground woody roots

[a]Ash trees with a tipping (TR) and/or breaking risk (BR). The degree of crown defoliation may have an unknown effect on the wind loads during a storm. Therefore, tipping and breaking risks are only valid in case this effect does not alter the wind loads significantly.
[b]Percentage of basal stem circumference covered by necroses.

4.3. *Armillaria* species associated with basal stem necroses

Of the five *Armillaria* species known to occur in Switzerland, four species (*A. borealis*, *A. cepistipes*, *A. gallica*, *A. mellea*), with *A. gallica* and *A. cepistipes* dominating, were isolated in this study from basal stem necroses on ash trees, which confirms previous reports (Lygis et al.,

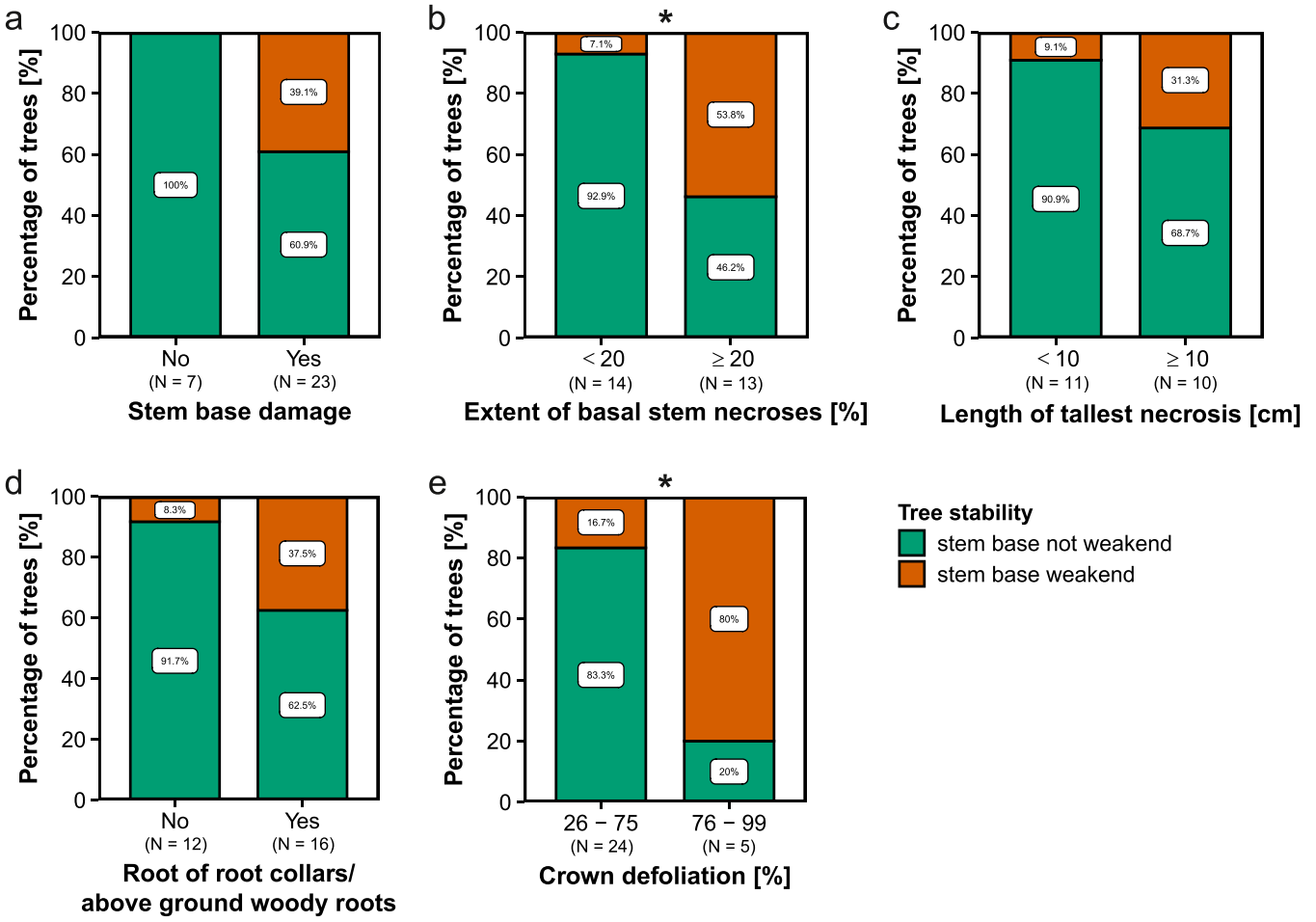

Fig. 7. Association of stem base damage and severity and crown defoliation with a weakness at stem base of ash trees (*Fraxinus excelsior*). (a) damage of the stem base by any means (e.g. fungus induces necroses, damage by logging operations, …), (b) extent of basal stem necroses (= percentage of basal stem circumference covered by necroses), (c) length of tallest necrosis, (d) rot of root collars/above ground woody roots and (e) degree of crown defoliation. In (a) a tree with stem damage by a forestry vehicle is included, whereas this tree was excluded from the other figures. Trees with missing values were also excluded. Trees with no indication of a weakness at the stem base (TIS/BS ≥ 1 and BRS/BS ≥ 1) are colored in green and trees with a weakness at the stem base (TIS/BS < 1 and BRS/BS < 1) are colored in orange. * Fisher's exact test indicated a significant association between damage severity and tree stability at $p < 0.05$.

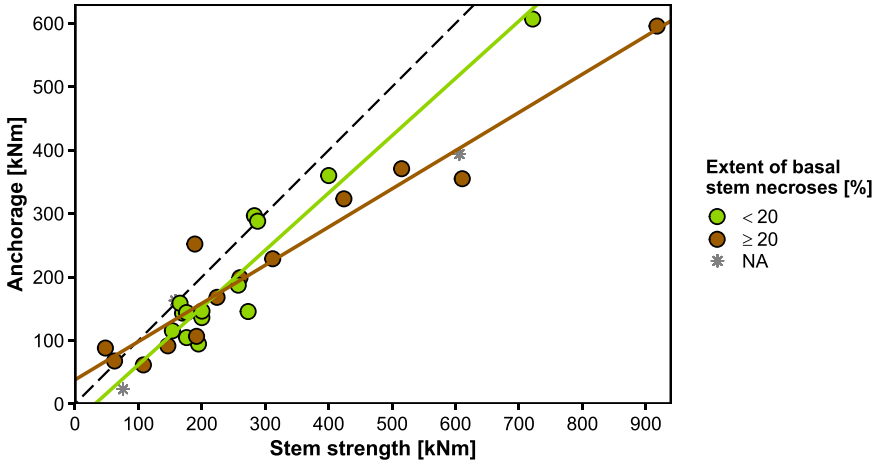

Fig. 8. Relationship between stem strength (BRS * estimated wind load) and anchorage (TIS * estimated wind load) for ash trees (*Fraxinus excelsior*) where the necroses covered < 20 % of the basal circumference (green dots, N = 14) and trees where the necroses covered ≥ 20 % of the basal circumference (brown dots, N = 13). Grey asterisks indicate trees where the extent of basal necroses was not recorded or which were heavily damaged by forestry vehicles. Those trees were excluded from the regression analysis. The dashed black line indicates a 1:1 relationship.

2005; Bakys et al., 2011; Husson et al., 2012; Enderle et al., 2013; Hauptman et al., 2016; Madsen et al., 2021; Peters et al., 2023). In agreement with studies from other European countries (Lygis et al., 2005; Bakys et al., 2011; Husson et al., 2012; Enderle et al., 2013; Hauptman et al., 2016; Madsen et al., 2021; Peters et al., 2023), *A. ostoyae*, which is widespread in Switzerland and central Europe where it often co-occurs with other *Armillaria* species (Guillaumin et al., 1993; Legrand et al., 1996; Rigling et al., 1998; Prospero et al., 2003b; Marxmüller and Guillaumin, 2005; Bendel et al., 2006; Dalya et al., 2019), was not found in any basal stem necrosis. Given the absence of *A. ostoyae* in the soil of the investigated Swiss ash stands, it could be that this species is not present at all or extremely rare in stations where common ash occurs. Indeed, *A. ostoyae* prefers coniferous hosts (Rishbeth, 1985; Blodgett and Worrall, 1992; Guillaumin et al., 1993). In contrast to *A. ostoyae*, *A. mellea* which was also never detected in the soil, was found in basal stem necroses in this study confirming previous investigations (Husson et al., 2012; Chandelier et al., 2016; Hauptman et al., 2016). Although *A. mellea* is a poor rhizomorph producer, it is frequently associated with broadleaved hosts (Rishbeth, 1985; Guillaumin et al., 1993), which may explain why it was occasionally found in ash trees.

On sites where *Armillaria* was collected from basal stem necroses as well as from the soil, *A. cepistipes* was more abundant in the soil than *A. gallica*, whereas the opposite was observed in basal stem necroses. Being the more virulent species (Guillaumin et al., 1993; Morrison, 2004), *A. gallica* as a secondary pathogen may have a competitive advantage over *A. cepistipes* in colonizing declining but still not dead ash trees. Alternatively, the prevalence of *A. gallica* in basal stem necroses could reflect its the higher affinity to broadleaf tree species (Blodgett and Worrall, 1992; Guillaumin et al., 1993)

Although in Europe the *Armillaria* species composition is changing with altitude and latitude (Marxmüller and Guillaumin, 2005), *Armillaria* occurs throughout the distribution range of ash, indicating that declining ash trees may not be able to escape *Armillaria*, but that species associated with basal stem necroses may vary, depending on the geographic location and/or altitude. In our study, for example, we observed that in Switzerland at higher altitudes ($\geq$ 600) *A. cepistipes* is replacing *A. gallica* and *A. mellea* in basal stem necroses, which were more common in basal stem necroses at lower altitudes.

4.4. Armillaria genets

The identification of *Armillaria* genets using microsatellite markers showed that more than half of the genets found as rhizomorphs in the soil or as epiphytic rhizomorphs at the tree base were also those infecting the ash trees. This finding confirms the ability of preferentially saprotrophic *Armillaria* species like *A. cepistipes* and *A. gallica* to produce dense perennial networks of rhizomorphs in the soil enveloping living trees, through which they rapidly capture (colonize) the trees as soon as they are weakened (Prospero et al., 2003a). Such networks are not only present around trees or stumps, but frequently cover the entire forest stand (e.g., Prospero et al., 2003b), which explains why in our study the prevalence of the two species in the soil was not affected by the distance from the sampled ash trees.

The higher diversity of *Armillaria* species and genets in basal stem necroses compared to the soil may indicate that our soil sampling grid was not dense enough to capture the entire diversity of the local *Armillaria* communities in the soil. On one side, we may have partially underestimated the incidence of species that are poor rhizomorph producers (e.g. *A. mellea*). On the other side, we probably missed small genets of *A. cepistipes* and *A. gallica* in the soil. Nevertheless, we were able to find 92.3 % of the *A. cepistipes* genets and 73.3 % of the *A. gallica* genets infecting ash trees also as soil or epiphytic rhizomorphs. Importantly, the soil sampling also revealed genets we did not detect in basal stem necroses. Therefore, as already shown in previous studies (Legrand et al., 1996; Prospero et al., 2003b), to assess species and genet diversity of *Armillaria* communities in forests, it is useful to sample *Armillaria* from infected trees as well as soil rhizomorphs.

4.5. Ash tree stability

At the end of the monitoring of the core plots in 2022, more than 75 % of the ash trees showed basal stem necroses, and, hence, were potentially suffering from advanced root rot. Nine out of 30 ash trees on which the non-destructive static load tests were carried out showed a weakness at the stem base, including a tree previously damaged by a forestry vehicle. The static load tests identified an increased risk of failure for six trees under the presumption that the effect of crown defoliation on drag in a storm did not reduce the wind loads significantly. Overall, the static load tests showed an increased level of weakening at the stem base with increasing damage severity at stem base and in the root collars and above ground woody roots. Although predicting weakness at the stem base from crown defoliation level and stem base damage level is not simple, i.e. also trees with advanced crown defoliation and stem necrosis can still be stable, our study shows that ash trees with necroses affecting at least 20 % of the basal stem circumference and trees with more than 75 % crown defoliation have a greater degree of weakening at the stem base and presumably an elevated risk of wind failure. Congruent with our findings, Enderle et al. (2017b) suggested, without having direct evidence, that ash trees with rot on more than 20 % of the cross-section area, which roughly corresponds to 20 % of necrotic circumference, assuming necroses have advanced cone-shaped from the bark to the stem center, may have stability issues and may pose a safety risk. In addition, our results align well with the pragmatic recommendations of Skovsgaard et al. (2017) who suggested to remove trees with crown defoliation exceeding 75 %, and that ash trees with little crown defoliation and a negligible amount of basal stem necroses (5–10 %), may be retained, if they are regularly inspected.

For all trees together the BRS and TIS were highly correlated. But our results show that for trees with necroses covering $\geq$ 20 % of the basal circumference, the ratio of anchorage and bending strength was different from trees with less necroses at the stem base. In particular stronger trees ($>$ 200 kNm) with necroses covering $\geq$ 20 % of the basal circumference were less resistant to failure by uprooting than by fracture at the stem base.

How quickly ash trees with basal stem necroses, colonized or not by *Armillaria*, may become a safety risk, is still poorly investigated. Based on the more than 20 %-cross-section-rot-criterium, Enderle et al. (2017b) suggested that some ash trees were already posing a risk within two years after basal stem necrosis formation, and that within five years after basal stem necrosis formation 41.7 % of ash trees were potentially hazardous. Conducting static load tests on the same set of ash trees and assessing the development of the basal stem necroses over subsequent years may be one way to shed further light on the trajectory of stability decline of ash trees, once basal stem necroses are present

4.6. Guidelines for management of mature ash trees and breeding

Although this study does not provide conclusive and completely scientifically sound criteria to evaluate the safety risk of mature ash trees based on crown status and basal stem health, it helps in developing pragmatic guidelines. Generally, it is desirable to retain or even promote apparently tolerant/resistant ash trees wherever it is possible to maintain the species persistence and genetic diversity (Skovsgaard et al., 2017). In non-risk situations for people and human infrastructures, there may not be an immediate need to remove highly deteriorated or dead ash trees as they may serve as habitat for organisms associated with ash or dead wood (Mitchell et al., 2014). For the risk assessment of an ash tree, it is crucial to address both its crown decline and the extent of necrosis at the stem base. As shown here and in previous studies (Husson et al., 2012; Enderle et al., 2013), those factors may be more (situations with advanced decline) or less (situations with less advanced decline)

correlated.

In risk situations (forests with a strong recreational function or next to human infrastructure), we recommend removing ash trees with at least 50 % crown defoliation and/or necroses encompassing at least 20 % of the basal stem circumference. If basal stem necroses affect less than 20 % of the stem circumference, and/or if crown defoliation ranges between 25 % and 50 %, there may be no immediate need to remove the ash tree, but regular inspections are recommended, as stem and root rot may advance quickly, especially if *Armillaria* spp. is involved. Ash trees with an undamaged stem base and less than 25 % crown defoliation can be retained, but regular inspections are also recommended.

For breeding of tolerant/resistant ash trees, not only resistance to crown dieback should be considered, but also the resistance to basal stem necroses, as root rot and rot of the basal stem considerably impact tree stability. In addition, basal stem necroses frequently serve as an entry point for *Armillaria* spp. which accelerate the rotting, and hence stability loss and tree mortality. Although resistance to crown dieback and basal stem necroses are heritable traits, they are genetically only moderately correlated (Muñoz et al., 2016), indicating that separate selections schemes may be required. Nevertheless, we assume that ash trees with healthier crowns, are generally more vigorous and should be better able to withstand attacks of secondary pathogens like *Armillaria* spp.

CRediT authorship contribution statement

Philipp Spiegel: Writing – original draft, Visualization, Methodology, Investigation, Formal analysis, Data curation. **Thomas Hintze**: Writing – review & editing, Investigation. **Aaron Kopp**: Writing – review & editing, Visualization, Investigation. **Mario Sahli**: Writing – review & editing, Investigation. **Andreas Detter**: Writing – review & editing, Software, Methodology, Data curation. **Valentin Queloz**: Writing – review & editing, Funding acquisition, Conceptualization. **Simone Prospero**: Writing – review & editing, Funding acquisition, Conceptualization. **Renate Heinzelmann**: Writing – review & editing, Writing – original draft, Visualization, Supervision, Project administration, Methodology, Investigation, Funding acquisition, Formal analysis, Data curation, Conceptualization.

Declaration of Competing Interest

The authors declare that they have no known competing financial interests or personal relationships that could have appeared to influence the work reported in this paper.

Acknowledgements

We thank the following persons for their help with the field assessments and the collection of *Armillaria* samples: Junia Koller, Sezer Olivia Kaya, José Ignacio Bustamante, Max Philippi, Federico Monteleone and Thibault Lachat and the students participating in his class “Forest protection and forest health” at the School of Agricultural, Forest and Food Sciences (HAFL), Zollikofen, Switzerland. We are also grateful to Samuel Buchle who conducted the static load tests together with Thomas Hintze. We also thank Robin Winiger, Sven Ulrich and Leandra Fritsi for their support with the molecular lab work. This project was funded by a grant from the Swiss Federal Office for the Environment FOEN (grant no. 00.5053.PZ/4D824FCB5). Finally, we thank the three reviewers for valuable comments on the manuscript.

Appendix A. Supporting information

Supplementary data associated with this article can be found in the online version at doi:10.1016/j.foreco.2024.122476.

Data availability

Data will be made available on request.

References

Anagnostakis, S.L., 1987. Chestnut blight: the classical problem of an introduced pathogen. Mycologia 79, 23–37.
Bakys, R., Vasiliauskas, A., Ihrmark, K., Stenlid, J., Menkis, A., Vasaitis, R., 2011. Root rot, associated fungi and their impact on health condition of declining *Fraxinus excelsior* stands in Lithuania. Scand. J. For. Res. 26, 128–135.
Bass, D., Stentiford, G.D., Wang, H.-C., Koskella, B., Tyler, C.R., 2019. The pathobiome in animal and plant diseases. Trends Ecol. Evol. 34, 996–1008.
Baumgartner, K., Grubisha, L.C., Fujiyoshi, P., Garbelotto, M., Bergemann, S.E., 2009. Microsatellite markers for the diploid basidiomycete fungus *Armillaria mellea*. Mol. Ecol. Resour. 9, 943–946.
Bendel, M., Kienast, F., Rigling, D., 2006. Genetic population structure of three *Armillaria* species at the landscape scale: a case study from Swiss *Pinus mugo* forests. Mycol. Res. 110, 705–712.
Blodgett, J.T., Worrall, J.J., 1992. Distributions and hosts of *Armillaria* species in New York. Plant Dis. 76, 166–170.
Brudi, E., van Wassenaer, P., 2002. Trees and statics: nondestructive failure analysis. In: Smiley, E.T., Coder, K.D. (Eds.), How trees stand up and fall down. Proceedings of the tree structure and mechanics conference. International Society of Arboriculture, Savannah, GA, pp. 53–70.
Carroll, D., Boa, E., 2024. Ash dieback: from Asia to Europe. Plant Pathol. 73, 741–759.
Chandelier, A., Gerarts, F., San Martin, G., Herman, M., Delahaye, L., 2016. Temporal evolution of collar lesions associated with ash dieback and the occurrence of *Armillaria* in Belgian forests. For. Pathol. 46, 289–297.
Core Team, R., 2023. R: A language and environment for statistical computing. R foundation for statistical computing, Vienna, Austria.
Cornejo, C., Kupper, Q., Queloz, V., 2024. An economic and reliable PCR approach to distinguish the primary pathogens *Armillaria mellea* and *A. ostoyae* from other European *Armillaria* species. J. Phytopathol. 172, e13429.
Cristini, V., Nop, P., Zlámal, J., Tippner, J., 2024. Incipient decay in beech (*Fagus sylvatica* L.) and linden (*Tilia cordata* Mill.): an interspecific static and dynamic material analysis. For. Ecol. Manag. 566, 122101.
Dalya, L., Capretti, P., Ghelardini, L., Jankovsky, L., 2019. Assessment of presence and distribution of *Armillaria* and *Heterobasidion* root rot fungi in the forest of Vallombrosa (Apennines Mountains, Italy) after severe windstorm damage. iForest - Biogeosciences For. 12, 118–124.
Denman, S., Doonan, J., Ransom-Jones, E., Broberg, M., Plummer, S., Kirk, S., Scarlett, K., Griffiths, A.R., Kaczmarek, M., Forster, J., Peace, A., Golyshin, P.N., Hassard, F., Brown, N., Kenny, J.G., McDonald, J.E., 2017. Microbiome and infectivity studies reveal complex polyspecies tree disease in acute oak decline. ISME J. 12, 386–399.
Detter, A., Richter, K., Rust, C., Rust, S., 2015. Aktuelle Untersuchungen zum Primärversagen von grünem Holz. In: Dujesiefken, D. (Ed.), Jahrbuch der Baumpflege 2015. Haymarket Media, Braunschweig, pp. 156–167.
Detter, A., Rust, S., Krišāns, O., 2023. Experimental test of non-destructive methods to assess the anchorage of trees. Forests 14, 533.
Detter, A., Rust, S., 2013. Aktuelle Untersuchungsergebnisse zu Zugversuchen. In: Dujesiefken, D. (Ed.), Jahrbuch der Baumpflege 2013. Haymarket Media, Braunschweig, pp. 87–100.
Detter, A., Rust, S., 2018. Grundlagen und Kriterien zur visuellen Beurteilung der Standsicherheit von Bäumen. In: Dujesiefken, D. (Ed.), Jahrbuch der Baumpflege 2018. Haymarket Media, Braunschweig, pp. 145–160.
Dorken, M.E., Eckert, C.G., 2001. Severely reduced sexual reproduction in northern populations of a clonal plant, *Decodon verticillatus* (Lythraceae). J. Ecol. 89, 339–350.
Drakulic, J., Gorton, C., Perez-Sierra, A., Clover, G., Beal, L., 2017. Associations between *Armillaria* species and host plants in UK gardens. Plant Dis. 101, 1903–1909.
Enderle, R., Busskamp, J., Metzler, B., 2017a. Growth performance of dense natural regeneration of *Fraxinus excelsior* under attack of the ash dieback agent *Hymenoscyphus fraxineus*. Balt. For. 23, 218–228.
Enderle, R., Peters, F., Nakou, A., Metzler, B., 2013. Temporal development of ash dieback symptoms and spatial distribution of collar rots in a provenance trial of *Fraxinus excelsior*. Eur. J. For. Res. 132, 865–876.
Enderle, R., Sander, F., Metzler, B., 2017b. Temporal development of collar necroses and butt rot in association with ash dieback. iForest - Biogeosciences For. 10, 529–536.
Engesser, R., Queloz, V., Meier, F., Kowalski, T., Holdenrieder, O., 2009. Das Triebsterben der Esche in der Schweiz. Wald. und Holz 90, 24–27.
Eschen, R., Kadzamira, M., Stutz, S., Ogunmodede, A., Djeddour, D., Shaw, R., Pratt, C., Varia, S., Constantine, K., Williams, F., 2023. An updated assessment of the direct costs of invasive non-native species to the United Kingdom. Biol. Invasions 25, 3265–3276.
Fensham, R.J., Radford-Smith, J., 2021. Unprecedented extinction of tree species by fungal disease. Biol. Conserv. 261, 109276.
Fuchs, S., Häuser, H., Peters, S., Knauf, L., Rentschler, F., Kahlenberg, G., Kätzel, R., Evers, J., Paar, U., Langer, G.J., 2024. Ash dieback assessments on intensive monitoring plots in Germany: influence of stand, site and time on disease progression. J. Plant Dis. Prot.
Gini, C., 1912. Variabilità e mutabilità: contributo allo studio delle distribuzioni e delle relazioni statistiche. Tipografia di Paolo Cuppini, Bologna.

Grosdidier, M., Scordia, T., Ioos, R., Marçais, B., 2020. Landscape epidemiology of ash dieback. J. Ecol. 108, 1789–1799.
Gross, A., Blaser, S., Senn-Irlet, B.J., 2024. SwissFungi: National data- and information center for the fungi of Switzerland, version 2 [database]. ⟨https://www.wsl.ch/map_fungi⟩. (accessed 16 Juli 2024).
Gross, A., Holdenrieder, O., Pautasso, M., Queloz, V., Sieber, T.N., 2014. *Hymenoscyphus pseudoalbidus*, the causal agent of European ash dieback. Mol. Plant Pathol. 15, 5–21.
Guillaumin, J.J., Mohammed, C., Anselmi, N., Courtecuisse, R., Gregory, S.C., Holdenrieder, O., Intini, M., Lung, B., Marxmüller, H., Morrison, D.J., Rishbeth, J., Termorshuizen, A.J., Tirro, A., Vandam, B., 1993. Geographical distribution and ecology of the *Armillaria* species in western Europe. Eur. J. For. Pathol. 23, 321–341.
Hauptman, T., Ogris, N., de Groot, M., Piškur, B., Jurc, D., 2016. Individual resistance of *Fraxinus angustifolia* clones to ash dieback. For. Pathol. 46, 269–280.
Heinzelmann, R., Dutech, C., Tsykun, T., Labbé, F., Soularue, J.-P., Prospero, S., 2019. Latest advances and future perspectives in *Armillaria* research. Can. J. Plant Pathol. 41, 1–23.
Heinzelmann, R., Prospero, S., Rigling, D., 2017. Virulence and stump colonization ability of *Armillaria borealis* on norway spruce seedlings in comparison to sympatric *Armillaria* species. Plant Dis. 101, 470–479.
Hothorn, T., Bretz, F., Westfall, P., 2008. Simultaneous inference in general parametric models. Biom. J. 50, 346–363.
Hothorn, T., Hornik, K., van de Wiel, M.A., Zeileis, A., 2006. A Lego system for conditional inference. Am. Stat. 60, 257–263.
Husson, C., Caël, O., Grandjean, J.P., Nageleisen, L.M., Marçais, B., 2012. Occurrence of *Hymenoscyphus pseudoalbidus* on infected ash logs. Plant Pathol. 61, 889–895.
Ioos, R., Fourrier, C., 2011. Validation and accreditation of a duplex real-time PCR test for reliable in planta detection of *Chalara fraxinea*. EPPO Bull. 41, 21–26.
Ioos, R., Kowalski, T., Husson, C., Holdenrieder, O., 2009. Rapid in planta detection of *Chalara fraxinea* by a real-time PCR assay using a dual-labelled probe. Eur. J. Plant Pathol. 125, 329–335.
Karadžić, D., Stanivuković, Z., Milanović, S., Sikora, K., Radulović, Z., Račko, V., Kardošová, M., Ďurkovič, J., Milenković, I., 2020. Development of *Neonectria punicea* pathogenic symptoms in juvenile *Fraxinus excelsior* trees. Front. Plant Sci. 11.
Kelley, M.B., Fierke, M.K., Stephen, F.M., 2009. Identification and distribution of Armillaria species associated with an oak decline event in the Arkansas Ozarks. For. Pathol. 39, 397–404.
Kim, M.-S., Heinzelmann, R., Labbé, F., Ota, Y., Elías-Román, R.D., Pildain, M.B., Stewart, J.E., Woodward, S., Klopfenstein, N.B., 2022. Chapter 20 - *Armillaria* root diseases of diverse trees in wide-spread global regions. In: Asiegbu, F.O., Kovalchuk, A. (Eds.), Forest Microbiology. Academic Press, London/Oxford/Cambridge MA/San, Diego, pp. 361–378.
Klesse, S., von Arx, G., Gossner, M.M., Hug, C., Rigling, A., Queloz, V., 2020. Amplifying feedback loop between growth and wood anatomical characteristics of *Fraxinus excelsior* explains size-related susceptibility to ash dieback. Tree Physiol. 41, 683–696.
Koeser, A.K., Thomas Smiley, E., Hauer, R.J., Kane, B., Klein, R.W., Landry, S.M., Sherwood, M., 2020. Can professionals gauge likelihood of failure? – Insights from tropical storm Matthew. Urban For. Urban Green. 52, 126701.
Lamichhane, J.R., Venturi, V., 2015. Synergisms between microbial pathogens in plant disease complexes: a growing trend. Front. Plant Sci. 6.
Langer, G., 2017. Collar rots in forests of Northwest Germany affected by ash dieback. Balt. For. 23, 4–19.
Legrand, P., Ghahari, S., Guillaumin, J.-J., 1996. Occurrence of genets of *Armillaria* spp. in four mountain forests in Central France: the colonization strategy of *Armillaria ostoyae*. N. Phytol. 133, 321–332.
Lenz, H.D., Bartha, B., Straßer, L., Lemme, H., 2016. Development of ash dieback in south-eastern Germany and the increasing occurrence of secondary pathogens. Forests 7, 41.
Lenz, H.D., Straßer, L., Baumann, M., Baier, U., 2012. Boniturschlüssel zur einstufung der vitalität von alteschen. AFZ-DerWald 3, 18–19.
Lygis, V., Vasiliauskas, R., Larsson, K.-H., Stenlid, J., 2005. Wood-inhabiting fungi in stems of *Fraxinus excelsior* in declining ash stands of northern Lithuania, with particular reference to *Armillaria cepistipes*. Scand. J. For. Res. 20, 337–346.
Madsen, C.L., Kosawang, C., Thomsen, I.M., Hansen, L.N., Nielsen, L.R., Kjær, E.D., 2021. Combined progress in symptoms caused by *Hymenoscyphus fraxineus* and *Armillaria species*, and corresponding mortality in young and old ash trees. For. Ecol. Manag. 491, 119177.
Manion, P.D., 1991. Tree Disease Concepts. Prentice Hall, Upper Saddle River, NJ.
Maphosa, L., Wingfield, B.D., Coetzee, M.P.A., Mwenje, E., Wingfield, M.J., 2006. Phylogenetic relationships among *Armillaria* species inferred from partial elongation factor 1-alpha DNA sequence data. Australas. Plant Pathol. 35, 513–520.
Marçais, B., Husson, C., Caël, O., Collet, C., Dowkiw, A., Saintonge, F.-X., Delahaye, L., Chandelier, A., 2017. Estimation of ash mortality induced by *Hymenoscyphus fraxineus* in France and Belgium. Balt. For. 23, 159–167.
Marçais, B., Husson, C., Godart, L., Caël, O., 2016. Influence of site and stand factors on *Hymenoscyphus fraxineus*-induced basal lesions. Plant Pathol. 65, 1452–1461.
Marxmüller, H., Guillaumin, J.J., 2005. Description et distribution des armillaires européennes. In: Guillaumin, J.J., Legrand, P., Lung-Escarmant, B., Botton, B. (Eds.), L'armillaire et le pourridié-agaric des végétaux ligneux. INRA, Paris, pp. 63–84.
Meyn, R., Langer, G.J., Gross, A., Langer, E.J., 2019. Fungal colonization patterns in necrotic rootstocks and stem bases of dieback-affected *Fraxinus excelsior* L. For. Pathol. 49, e12520.
Mitchell, R.J., Beaton, J.K., Bellamy, P.E., Broome, A., Chetcuti, J., Eaton, S., Ellis, C.J., Gimona, A., Harmer, R., Hester, A.J., Hewison, R.L., Hodgetts, N.G., Iason, G.R., Kerr, G., Littlewood, N.A., Newey, S., Potts, J.M., Pozsgai, G., Ray, D., Sim, D.A., Stockan, J.A., Taylor, A.F.S., Woodward, S., 2014. Ash dieback in the UK: A review of the ecological and conservation implications and potential management options. Biol. Conserv. 175, 95–109.
Morrison, D.J., 2004. Rhizomorph growth habit, saprophytic ability and virulence of 15 *Armillaria* species. For. Pathol. 34, 15–26.
Mulholland, V., MacAskill, G.A., Laue, B.E., Steele, H., Kenyon, D., Green, S., 2012. Development and verification of a diagnostic assay based on EF-1 a for the identification of *Armillaria* species in Northern Europe. For. Pathol. 42, 229–238.
Muñoz, F., Marçais, B., Dufour, J., Dowkiw, A., 2016. Rising out of the ashes: additive genetic variation for crown and collar resistance to *Hymenoscyphus fraxineus* in *Fraxinus excelsior*. Phytopathology® 106, 1535–1543.
Peet, R.K., 1974. The measurement of species diversity. Annu. Rev. Ecol. Syst. 5, 285–307.
Peters, S., Fuchs, S., Bien, S., Bußkamp, J., Langer, G.J., Langer, E.J., 2023. Fungi associated with stem collar necroses of *Fraxinus excelsior* affected by ash dieback. Mycol. Prog. 22, 52.
Pommnitz, M., 2016. Mangelnde Standsicherheit von Bäumen nach Baumaßnahmen - Gründe für einen sinvollen Baumschutz. In: Dujesiefken, D. (Ed.), Jahrbuch der Baumpflege 2016. Haymarket Media, Braunschweig, pp. 183–190.
Prospero, S., Holdenrieder, O., Rigling, D., 2003a. Primary resource capture in two sympatric *Armillaria* species in managed Norway spruce forests. Mycol. Res. 107, 329–338.
Prospero, S., Holdenrieder, O., Rigling, D., 2004. Comparison of the virulence of *Armillaria cepistipes* and *Armillaria ostoyae* on four Norway spruce provenances. For. Pathol. 34, 1–14.
Prospero, S., Jung, E., Tsykun, T., Rigling, D., 2010. Eight microsatellite markers for *Armillaria cepistipes* and their transferability to other *Armillaria* species. Eur. J. Plant Pathol. 127, 165–170.
Prospero, S., Rigling, D., Holdenrieder, O., 2003b. Population structure of *Armillaria* species in managed Norway spruce stands in the Alps. N. Phytol. 158, 365–373.
Queloz, V., Hopf, S.-E., Schoebel, C., Rigling, D., Gross, A., 2017. Ash dieback in Switzerland: history and scientific achievements. In: Vasaitis, R., Enderle, R. (Eds.), Dieback of European Ash (*Fraxinus* spp.). Consequences and guidelines for sustainable management. SLU, Uppsala, pp. 68–78.
Quirion, B.R., Domke, G.M., Walters, B.F., Lovett, G.M., Fargione, J.E., Greenwood, L., Serbesoff-King, K., Randall, J.M., Fei, S., 2021. Insect and disease disturbances correlate with reduced carbon sequestration in forests of the contiguous United States. Front. For. Glob. Change 4.
Rigling, D., Blauenstein, H., Walthert, L., Rigling, A., Kull, P., Schwyzer, A., Heiniger, U., 1998. Rhizomorph producing Armillaria species in Norway spruce stands in Switzerland. In: Delatour, C., Marçais, B., Guillaumin, J.J., Lung-Escarmant, B. (Eds.), Root and Butt Rots of Forest Trees - 9th International Conference on Root and Butt Rots. INRA, Paris, pp. 259-265.
Rishbeth, J., 1985. Infection cycle of *Armillaria* and host response. Eur. J. For. Pathol. 15, 332–341.
Robbins, Z.J., Xu, C., Aukema, B.H., Buotte, P.C., Chitra-Tarak, R., Fettig, C.J., Goulden, M.L., Goodsman, D.W., Hall, A.D., Koven, C.D., Kueppers, L.M., Madakumbura, G.D., Mortenson, L.A., Powell, J.A., Scheller, R.M., 2022. Warming increased bark beetle-induced tree mortality by 30% during an extreme drought in California. Glob. Change Biol. 28, 509–523.
Rust, S., van Wassenaer, P., 2017. Tools for tree risk assessment. Managing urban forsts and urban trees. In: Fini, A., Konijnendijk van den Bosch, C.C., Ferrini, F. (Eds.), Routledge Handbook of Urban Forestry. Routledge, Abingdon-on-Thames, pp. 489–499.
Sachverständigenarbeitsgemeinschaft (SAG) Baumstatik E.V., 2024. Standards of the SAG Baumstatik Group for the application of the pulling test according to the static load test method (SIM). SAG pulling test standards. 1st Edition. SAG Baumstatik e.V., Gauting.
Santini, A., Ghelardini, L., De Pace, C., Desprez-Loustau, M.L., Capretti, P., Chandelier, A., Cech, T., Chira, D., Diamandis, S., Gaitniekis, T., Hantula, J., Holdenrieder, O., Jankovsky, L., Jung, T., Jurc, D., Kirisits, T., Kunca, A., Lygis, V., Malecka, M., Marçais, B., Schmitz, S., Schumacher, J., Solheim, H., Solla, A., Szabò, I., Tsopelas, P., Vannini, A., Vettraino, A.M., Webber, J., Woodward, S., Stenlid, J., 2013. Biogeographical patterns and determinants of invasion by forest pathogens in Europe. N. Phytol. 197, 238–250.
Sinn, G., Wessolly, L., 1989. A contribution to the proper assessment of the strength and stability of trees. Arboric. J. 13, 45–65.
Skovsgaard, J.P., Wilhelm, G.J., Thomsen, I.M., Metzler, B., Kirisits, T., Havrdová, L., Enderle, R., Dobrowolska, D., Cleary, M., Clark, J., 2017. Silvicultural strategies for *Fraxinus excelsior* in response to dieback caused by *Hymenoscyphus fraxineus*. For.: Int. J. For. Res. 90, 455–472.
Smiley, E.T., Matheny, N.P., Lilly, S., 2017. Best management practices: tree risk assessment. International Society of Arboriculture, Atlanta, GA.
Teshome, D.T., Zharare, G.E., Naidoo, S., 2020. The threat of the combined effect of biotic and abiotic stress factors in forestry under a changing climate. Front. Plant Sci. 11.
Tsykun, T., Rigling, D., Prospero, S., 2013. A new multilocus approach for a reliable DNA-based identification of *Armillaria* species. Mycologia 105, 1059–1076.
Vollsinger, S., Mitchell, S.J., Byrne, K.E., Novak, M.D., Rudnicki, M., 2005. Wind tunnel measurements of crown streamlining and drag relationships for several hardwood species. Can. J. For. Res. 35, 1238–1249.
van Wassenaer, P., Richardson, M., 2009. A review of tree risk assessment using minimally invasive technologies and two case studies. Arboric. J. 32, 275–292.
Watson, J.E.M., Evans, T., Venter, O., Williams, B., Tulloch, A., Stewart, C., Thompson, I., Ray, J.C., Murray, K., Salazar, A., McAlpine, C., Potapov, P., Walston, J., Robinson, J.G., Painter, M., Wilkie, D., Filardi, C., Laurance, W.F., Houghton, R.A., Maxwell, S., Grantham, H., Samper, C., Wang, S., Laestadius, L., Runting, R.K., Silva-

Chávez, G.A., Ervin, J., Lindenmayer, D., 2018. The exceptional value of intact forest ecosystems. Nat. Ecol. Evol. 2, 599–610.
Wessolly, L., 1995. Bruchdiagnose von Bäumen - Teil 2: Statisch integrierte Verfahren - Die statisch integrierte Abschätzung (SIA). Stadt. und Gr. üN. 95/8, 570–573.
Wessolly, L., 1996. Standsicherheit von Bäumen. Der Kippvorgang ist geklärt. Stadt. und Gr. üN. 96 (4), 268–272.
Wessolly, L., Erb, M., 2016. Manual of tree statics and tree inspection. Patzer Verlag, Berlin.
White, T.J., Bruns, T.D., Lee, S.B., Taylor, J.W., 1990. Amplification and direct sequencing of fungal ribosomal RNA genes for phylogenetics. In: Innis, M.A., Gelfand, D.H., Sninsky, J.J., White, T.J. (Eds.), PCR - Protoc. Appl. - A Lab. Man. Acad. Press, N. Y. 315–322.
Xu, P., Guan, C., Zhang, H., Li, G., Zhao, D., Ross, R.J., Shen, Y., 2021. Application of nondestructive testing technologies in preserving historic trees and ancient timber structures in China. Forests 12, 318.